MARSOL

Demonstrating Managed Aquifer Recharge as a Solution to Water Scarcity and Drought

Llobregat Demonstration Site - Laboratory Tests: Developments and Modelling

Deliverable No.	D6.3
Version	1
Version Date	04.11.2016
Author(s)	Xavier Sanchez-Vila, Paula Rodríguez-Escales, Albert Carles-Brangarí (UPC)
	Contact: xavier.sanchez-vila@upc.edu
Dissemination Level	PU
Status	Final

Contents:

EXECUTIVE SUMMARY

This is the third deliverable in WP 6 aimed at improving groundwater quantity and quality by discharging river water through infiltration basins located in the Lower Valley of the Llobregat River in Catalonia, Spain. Deliverable 6.3 reflects some recent work in laboratory experiments and modelling.

The work is composed by two main contributions. In the first one we present the results of an 83-day long mesocosm infiltration experiment, aiming at analyzing microbial functions such as extracellular enzyme activities and carbon substrate utilization in the sediment profile, and determining organic matter use under different oxygenic conditions. We found that the surface sediment layers were colonized by microorganisms capable of using a wide range of substrates (although they preferred to degrade carbon polymeric compounds). In contrast, at a depth of 50 cm, the microbial community became specialized and used fewer carbon substrates, showing decreased functional richness and diversity. At this depth, microorganisms picked nitrogenous compounds, including amino acids and carboxyl acids. After the 83-day experiment, the sediment at the bottom of the column showed reduced dissolved oxygen concentrations. The presence of specific metabolic fingerprints under oxic and anoxic conditions indicated that the microbial community was adapting to use organic matter and adapt to the existing oxygen gradient. The experimental results indicate that heterogeneous oxygen conditions influence organic matter metabolism in a sediment column.

In the second part of the deliverable, we first compile all the existing experimental data to formulate a comprehensive degradation model of the antibiotic sulfamethoxazole (SMX) in aquifers under varying redox conditions, ranging from aerobic to iron reducing conditions. Depending on the redox state, SMX degrades reversibly or irreversibly to a number of metabolites that are specific of that particular state. Reactions are in all cases biologically mediated. We then propose a mathematical model that reproduces the fate of dissolved SMX subject to anaerobic conditions and that can be used as a first step in emerging compound degradation modelling efforts. The model presented is

satisfactorily tested against the results of the batch experiments of Barbieri et al. (2012) and Nödler et al. (2012) displaying a non-monotonic concentration of SMX as a function of time under denitrification conditions, as well as those of Mofatt et al. (2011), under iron reducing conditions, providing results that support the model proposed.

1 Introduction

1.1 Objective

This is the third deliverable in the Work Package entitled DEMO Site 4: Llobregat River Infiltration Basins, Sant Vicenç dels Horts, Catalonia, Spain. Here river water is infiltrated into the ground to increase water resources. We test the role of microbial communities (in terms of present biofilm) that on one hand reduces the total amount of infiltration (pore bioclogging), and on the other is capable of reduce the observed concentrations of pharmaceuticals and other emerging compounds found in the river water, coming from discharges by WWTPs.

The main objective of Deliverable 6.3 is to reflect our recent work in laboratory experiments performed with soil material from the MARSOL Demo Site of Sant Vicenç dels Horts, with emphasis in the biogeochemical modelling aspects.

1.2 Outline

The work is composed on two experiments. The first one, presented in Chapter 2, involves an infiltration experiment in a vertical tank, and concentrates on the analysis of the changes in organic matter use as a function of depth, with emphasis in the microbiological colonies found at different depths. The second one, in Chapter 3, involves the interpretation by modelling of the very non-linear degradation process of an emerging organic compound linked to denitrification.

2 Changes in organic matter use in an infiltration sediment experiment according to depth and oxygen concentration

2.1 Introduction

The processes taking place in the interface between surface water and groundwater during the infiltration process is important in Managed Aquifer Recharge activities. The vadose zone promotes the exchange of water, nutrients, and biota between the surface and the subsurface water bodies, with significant implications in water quality.

Microbial communities in soils are composed of heterotrophic microorganisms including bacteria, fungi, and small metazoans which are attached to sand grains and assembled in a polymeric matrix. Microbial communities are responsible for the metabolic activity in sediments, such as the degradation of organic matter and the reduction of electron acceptors (oxygen, nitrate and sulphate; see Ghiorse and Wilson, 1988; Hedin et al., 1998). Aquifer recharge may promote the development of microbial communities at different depths.

Percolation through a saturated zone is often used to enhance the quality of surface water (Greskowiak et al., 2005), although the microbial processes are not well defined. Decomposition of organic matter is one of the main metabolic roles of microorganisms in soils and sediments. Extracellular enzymes released by microbes promote organic carbon cycling, by transforming polymeric material into soluble monomers that can be assimilated. These actions are a limiting step in the entrance of organic matter to the food web (Romaní et al., 2012). The capacity of microorganisms to use and recycle organic compounds is also linked to diversity; higher functional heterogeneity and richness may be related to higher microbial diversity (Cardinale et al., 2006) and eventually to higher availability of organic compounds. Functional diversity promotes ecosystem function and increases the ability to cope with the changing availability of organic matter. Although many studies have analysed enzyme activities in surface sediments (Romaní and Sabater, 2001), little is known about how these activities change with depth.

Biomass is not homogeneously distributed in space. Microorganisms are found in largest quantities at the soil surface, and their abundance declines rapidly with depth (Taylor et al., 2002). Bacteria in deeper sediments are more sensitive to physical and chemical changes compared to those in surface layers due to the relatively more stable conditions in terms of oxygen, pH, temperature and nutrient availability (Fischer et al., 2005). Moreover, biofilms may create microenvironments that allow anaerobic processes to coexist within aerobic sediments (Harvey et al., 1995) indicating that anoxic environments can promote areas of organic matter preservation with slower rates of carbon decomposition.

The experimental work performed aimed at: i) analysing organic matter decomposition capabilities and microbial functional diversity of the community developed in depth as a result of colonization; and ii) investigating the vertical changes of organic matter use due to different oxygenic conditions.

2.2 Material and methods

2.2.1. Experimental design

An infiltration (flow-through) experiment was conducted in a vertical intermediate-scale tank reconstructed with a heterogeneous sediment porous media. The dimensions of the sediment tank were 1.20 m high × 0.45 m long × 0.15 m wide. The base of the tank was filled with a 15 cm layer of silicic sand (0.7 to 1.8 mm diameter, supplied by Triturados Barcelona, Inc.) covered with a permeable geo-synthetic fabric membrane to prevent soil flowing through. Sediments were collected from the MARSOL Demo Site located in the Llobregat River near Barcelona. Sediments were sieved at 0.5 cm and packed in the tank without further treatment. The top 20 cm of the tank were left free of sediment to allow ponding.

A concentrated synthetic solution of 10L mixture of inorganic and organic compounds was prepared in a carboy. This concentrated solution was diluted with deionized water prior to its injection into the infiltration pond of the tank. A

system of two pumps and a connecting valve ensured the proper mixing of the two fluids. The carboy solution was continuously mixed with a magnetic stirrer (AREX 230v/50Hz, VELP Scientific) and supplied at the surface of the tank with no recirculation. The carboy was replaced every 4-7 days (depending on water consumption). Water chemical composition of the mixture mimics the typical Llobregat River water is reported in Table 1. All tubes, valves and carboys were autoclaved and covered with a black foil prior to the start of the experiment.

Table 1. Synthetic water composition used as input water to the flow-through system during the experiment (from Fernandez-Turiel et al., 2003).

Synthetic water composition	
Compound	**mg/L**
$CHNaO_3$	160
KH_2PO_4	1.2
$MgCl_2\ 6H_2O$	211.7
$Mg(NO_3)_2\ 6H_2O$	20.0
KCl	60.0
$CaCl_2\ 2H_2O$	352.8
Na_2SO_4	240.0
NH_4Cl	4.0
Na_2SiO_3	16.0
Cellobiose	1.2
Leucine-proline	1.2
Humic acid	5.6

The upper layer in the tank was exposed to sunlight, while the lateral walls were covered with dark plastic to prevent photoautotrophic activity. At the beginning of the experiment, a microbial inoculum was added to the top of the tank to promote colonization. The inoculum was prepared from sediment collected at the pristine riverbed nearby the site. 20 mL of sediment extract from five core sediment samples (5 cm diameter, 5-10 cm depth) were added to the tank. This inoculum contained $2.27 \pm 0.41 \times 10^6$ bacterial cells/mL.

The tank was equipped with duplicate liquid ports at depths 5, 15, 30, 45 and 58 cm (all distances measured from the surface of the sediment). Sediment sampling ports consisting of 1.5 cm horizontal holes tapped with cork caps

located at 20 and 50 cm depth, samples were collected with a methacrylate corer (1.5 cm in diameter) displayed horizontally; samples from the surface were collected vertically. Despite sampling collection led to local changes in hydraulic conductivity right after sampling, the system used minimizes the overall impact as it readjusts quickly to fill the gap created. Then, subsamples of 0.5 mL of sediment were collected in triplicate with an uncapped syringe for each analysis.

2.2.2. Physical Analysis

Measured values of temperature and volumetric water content were recorded continuously by using capacitance sensors (5TE, Decagon Devices, Pullman, WA) placed at 3 different depths. A handheld multiparameter instrument (YSI Professional Plus) recorded temperature, electrical conductivity, dissolved oxygen and pH in continuous at the tank outlet. Sensors were recalibrated and checked daily. Dissolved oxygen concentrations were measured continuously with optical fibers (FiboxPresens, Germany) and corrected for temperature.

The evolution of infiltration rate (R) with time was determined from water balance considerations at the pond, resulting in the following equation:

$R(t) = I(t) - \Delta h / \Delta t$

where I(t) is the pumping rate per unit surface area at time t, and h(t) is the height of water at the pond. Direct evaporation was estimated, and found negligible to the overall balance.

2.2.3. Chemical Analysis

Inorganic nutrients were measured from the water samples collected at days 0, 3, 8, 13, 16, 20, 24, 28, 33, 36, 40, 43, 49, 53 and 83 at 5 depths (5, 15, 30, 45 and 58 cm measured from the surface). Water samples were collected in 9 mL vacuum vials and filtered at 0.2 μm (Whatman). Analysis for NO_3^-, NH_4^+ and Cl^- were performed by HPLC. Measurements of dissolved organic carbon (DOC) were obtained at the same depths as those of nutrients from the water

samples collected at days 13, 16, 20, 24, 28, 33, 36, 40, 43, 49, 53 and 83. Samples were filtered (Whatman GF/F), conditioned with 2M HCl and stored at 5°C until analyses were performed. DOC was measured using a total organic carbon analyser (Shimadzu TOC-V-CSH 230V, Tokyo, Japan). Three replicates were used for each sample. Phosphate (PO_4) was analysed spectrophotometrically, only at days 3, 13, 49 and 83 at 3 different depths (5, 15 and 45).

2.2.4. Biological Analysis

Microbial activity and bacterial abundance were analysed from sediment samples and were processed during the same sampling day. Samples for extracellular enzyme activities were collected on days 0, 3, 6, 9, 14, 21, 34, 50 and 83. Biolog EcoPlate incubations and bacterial abundance and viability were estimated on days 3, 14, 34, 50 and 83.

Bacterial abundance and viability

Live and dead bacteria in sediment were counted using a bacterial viability kit (Invitrogen Molecular Probes, Inc.). Each collected sediment subsample (1 mL of sand volume, 3 replicates) was placed in a sterile vial with 10 mL of Ringer solution (Scharlau S.L). Bacteria were detached from sediment after sonication for 1 min using an ultrasonic bath (Selecta, 40W, 40kHz). The extract was diluted (20 times at the beginning of the experiment, 50 times from day 14) with Ringer solution. The diluted sediment extract was used for bacterial density and viability analysis and also as the inoculum for the Biolog Ecoplates incubations.

For each diluted sediment extract, 2 mL were stained by a 1:1 mixture of Syto9 and PI and incubated for 15 min in dark conditions. Samples were filtered through a 0.2 µm pore-size black polycarbonate filters (GE Water and Process Technologies) and then mounted on a microscope slide. Twenty randomly chosen fields were counted for each slide for live and dead bacteria (Nikon E600 epifluorescence microscope, 1000X, Nikon Corporation, Tokyo, Japan).

Carbon substrate utilization profiles

Biolog Ecoplates (Biolog Inc., Hayward, CA, USA) were used to determine the differences in the metabolic fingerprint in time and depth of the sediment column based on carbon source utilization.

Each sampling day, the diluted sediment extracts from each depth (3 replicates per depth) were incubated in the Ecoplates for 5 h after sampling. Ecoplates were inoculated with 130 µL of sediment extract under sterile conditions and incubated at 20°C in dark conditions for 6 days. Plates were read every 24 h at 590 nm using a microplate reader (SynergyTM 4, BioTek, Winooski, VT, USA). After 144 h, most wells had achieved sigmoid colour development saturation and the AWCD (Average Well Colour Development) was close to 0.6. Raw absorbance data obtained from Biolog Ecoplates were corrected by the mean absorbance of the 3 control (no substrate) wells in each plate. Values < 0.05 (or negative) were set to zero.

Data from Ecoplates were analysed by calculating the AWCD, Shannon diversity index (H') and Substrate richness (S) to evaluate microbial community functional diversity and functional richness (Garland and Mills, 1991). Substrate richness is the number of different substrates used by the community (counting all positive OD readings). Kinetic analysis was carried out for AWCD for each time and depth. Three kinetic parameters (*a*, *1/b* and *x0*) were estimated by fitting the curve of colour development on plates to a sigmoid equation, where *a* is the maximum absorbance in the event of colour saturation, *1/b* is the slope of the maximum rate of colour development, and *x0* is the time when maximum colour development rate is achieved. To evaluate utilization of dissolved organic nitrogen compounds, the nitrogen use (NUSE) index was calculated as the proportion (in percentage) of the summed absorbance of those substrates that have C and N over the total absorbance measured in each Ecoplate.

Extracellular enzyme activities

Three extracellular enzyme activities were analysed in the sediment, linked to the capacity to decompose cellobiose (β-glucosidase activity, EC 3.2.1.21,

denoted by BG), peptides (leucine-aminopeptidase activity, EC 3.4.11.1, LEU) and phosphomonoesters (phosphatase activity, EC 3.1.3.1, PHO).

Extracellular enzyme activities were determined with a spectrofluorometer using artificial fluorescent substrates 4-methylumbelliferone (MUF)-β-D-glucoside, MUF-phosphate, and L-leucine-4-7-methylcoumarylamide (AMC), for BG, PHO, and LEU, respectively in triplicate for each time and depth. Sediment samples were placed in vials filled with 4 mL of filtered tank water (0.2 μm nylon, Whatman). Samples were incubated at saturation (concentration of 300 μM) conditions at 20ºC under continuous shaking (150 rpm) during 1 h in dark conditions. Blanks (with 0.2 μm filtered water from the tank) were also incubated to eliminate the background signals and water fluorescence. At the end of the incubation period, 4 mL of glycine buffer (pH 10.4) solution was added, and fluorescence was measured at 365/455 nm excitation/emission wave lengths for MUF and at 364/445 nm excitation/emission wave lengths for AMC (Kontron SFM 25, Munich, Germany). Standard curves (0-200 μmol/L) were prepared for MUF and AMC, separately. Activity values are expressed as nmol of AMC or MUF released per g DW of sediment per hour.

Extracellular enzymes and carbon substrate utilization under anoxic conditions

An extra set of samples from days 14, 34, 50 and 83, sampled at 50 cm depth were collected for Biolog Ecoplates and extracellular enzyme activity measurements under anoxic conditions. The analytical protocols were the same as those described above, except that the incubations were performed under an anoxic atmosphere and the collected samples and sediment extracts were purged with nitrogen gas at the moment of collection. The incubations for Biolog Ecoplates and extracellular enzyme activities were performed within a hermetic bottle in anoxic conditions (AnaeroGen system, Oxoid, UK). For the Biolog Ecoplates incubations, plates were covered with silicone sealing film (Sigma). Oxygen values were measured before and after incubations (WTW oxygen meter).

2.2.5. Data Analysis

Differences among depths and days for temperature, oxygen, extracellular enzymes, bacterial density and viability, and parameters obtained from carbon substrate utilization profiles (AWCD, Shannon diversity index, Richness, NUSE index and kinetic parameters) were tested using repeated measures analysis of variance (RM-ANOVA, depth and days as a factor). All variables were logarithmically transformed, except for AWCD and Shannon index and kinetic parameters to render symmetric variables.

Differences between depth observed on day 83 were further analysed using a one-way analysis of variance (ANOVA, depth as a factor) between enzyme activities, Biolog parameters (Shannon diversity index, Richness, NUSE index), total bacterial and live bacterial densities. Also, the differences between oxic and anoxic incubations for enzyme activities and Biolog Ecoplates analysis were analysed by analysis of variance (ANOVA, oxygen as a factor). Nutrients (NO_3^-, NH_4^+, and DOC) for each day and depth were analysed using a two-way analysis of variance (ANOVA, depth and time as factors). All data were previously logarithmically transformed. All of these statistical analyses were performed using the program SPSS v.15.0 (SPSS, Inc., Chicago, IL, USA) and differences were considered to be significant at $p < 0.05$.

The relationships between degrading enzymes (BG:LEU, BG:PHO, and LEU:PHO, as indicators of C:N, C:P and N:P, respectively) obtained under oxic and anoxic conditions were calculated in order to estimate potential imbalances in nutrient needs and capabilities. These enzyme ratios were estimated based on linear regression analysis of the natural log transformed enzyme activities. Results were expressed in terms of the slope and the coefficient of variation.

Non-metric multi-dimensional scaling (NMDS) ordination plots were performed to visualize the spatial distribution pattern of the metabolic profiles in time and depth obtained from the Biolog Ecoplates of the 31 carbon substrates as well as to distinguish between oxic and anoxic metabolic profiles obtained at 50 cm depth. A previous distance matrix with Bray-Curtis similarity was created. NMDS is based on the rank order relation of dissimilarities where the largest

distance between samples denotes the most different microbial functional profile. In addition, as suggested by Choi and Dobbs (1999), the 31 carbon sources in the plate were grouped in six functional categories including polymers, carbohydrates, carboxylic acids, phenolic compounds, amines, and amino acids. Based on these data, ANOSIM analysis (analysis of similarity) were performed using the "vegan" package in R software to test for differences between functional profiles in depth and time.

2.3 Results

2.3.1. Physicochemical parameters

Dissolved oxygen decreased at all depths after the start of the experiment, approaching values below 2 mg/L after day 34. Significant differences were observed among depths indicating lower oxygen concentration at the bottom of the tank ($p < 0.01$, Fig. 2.1). Based on oxygen data, three time periods were used for analyses of nutrient content and enzyme ratios.

Period 1 (P1): From day 1 to day 28; defined by the development of a clear oxygen gradient in depth with values of about 8 mg/L at the sediment surface and 4 mg/L at 50 cm in depth.

Period 2 (P2): From day 33 to day 53; defined by an oxygen gradient reduction leading to similar values in depth close to 4 mg/L.

Period 3 (P3): From day 64 to day 83; defined by a decrease in oxygen from values of about 4 mg/L to 2 mg/L in the first 20 cm of the sediment and to anoxic conditions at the bottom (depth of 50 cm).

Water temperature increased from 18.14 ± 0.10 ºC to 25.18 ± 0.14 ºC during the experiment, although no significant differences in temperature were observed among depths, indicating rapid re-equilibration with atmospheric conditions. The infiltration rate changed dynamically throughout the experiment, ranging from an initial value of 40 L/day to 15 L/day at day 83 (Fig. 2.1).
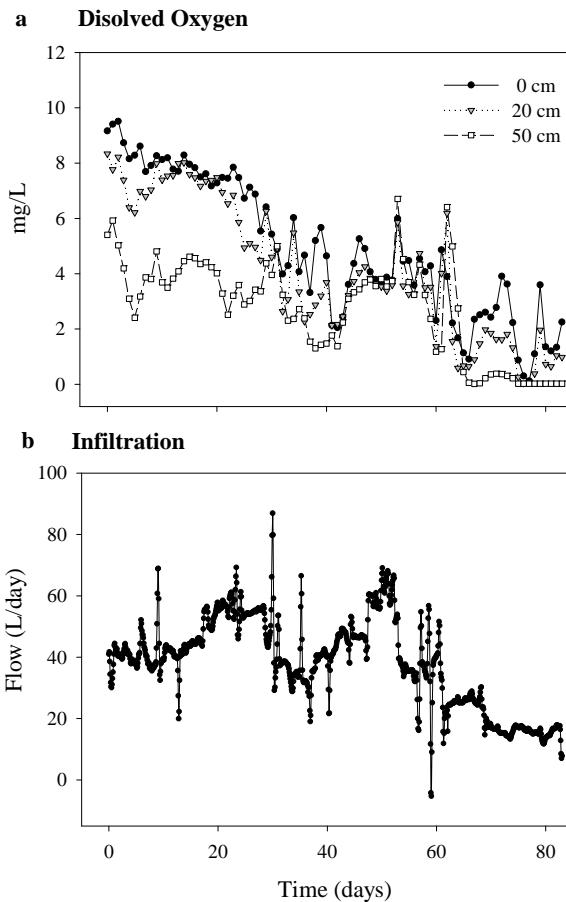
Figure 2.1. Temporal evolution of oxygen concentration and infiltration rates at three different depths. Values represent daily means, and had been corrected for changes in temperature.

The chemical composition of the interstitial water varied according to time and depth (Fig. 2.2), whereas the pH values remained relatively stable throughout the experiment (pH 7.6–8). Dissolved NO_3^- varied from 6 to 16 mg/L over time. NH_4^+ also varied according to depth and time, peaking at 1.5 mg/L during P1 and remaining below 0.05 mg/L after day 33. Dissolved organic carbon (DOC) values diminished over time, but was not influenced by depth. Chloride concentration remained stable over time and depth, ranging from 186 to 227 mg/L (Fig. 2.2). Inorganic phosphorous did not show any trend with depth; however a decrease of phosphate was observed at the end of the experiment: day 3 (0.27 ± 0.01), day 13 (0.41 ± 0.09), day 49 (0.38 ± 0.06) and day 83 (0.16 ± 0.03).
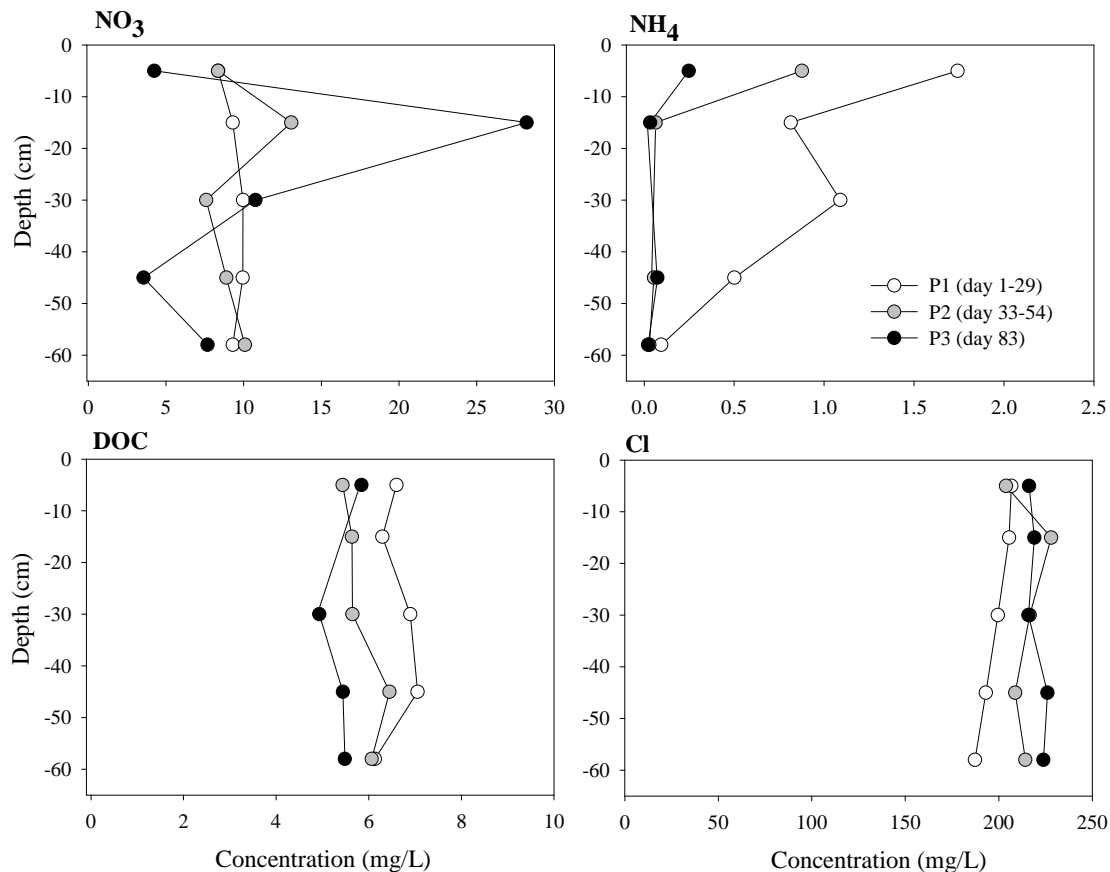
Figure 2.2. Mean values of nitrate (NO3-), ammonia (NH4+), organic carbon (DOC) and Chloride (Cl) at the three selected periods (P1, days 1 to 28; P2, days 33 to 53; P3, days 64 to 83) and as a function of depth.

2.3.2. Biological parameters

Bacterial abundance and viability

Bacterial density increased rapidly during the colonization process, with a mean maximum of 1.20×10^9 cells/g dry weight on day 83. No differences in bacterial density with depth were observed ($p > 0.05$, Table 3). Live bacteria accounted for 44.5% ± 7.1% of the average total bacteria for the whole experiment. The maximum value, 51.3%, was obtained at day 34 in surface sediment (Table 2). No differences were observed at different depths (not reported here).

Table 2. Bacterial density and live bacteria at different sampling dates and depths. Values are means (from 3 replicates) expressed as 10^9 cell/g of DW of sediment. Standard deviation is shown.

Days	Bacterial density			Live bacteria		
	0 cm	15 cm	50 cm	0 cm	15 cm	50 cm
3	0.11	0.07	nd	0.03	0.03	nd
14	0.19±0.04	0.36±0.01	0.29±0.03	0.09±0.01	0.15±0.02	0.12±0.01
34	1.96±0.25	1.23±0.07	1.41±0.03	1.17±0.16	0.47±0.04	0.78±0.03
50	1.39±0.18	1.08±0.03	1.11±0.30	0.58±0.11	0.39±0.03	0.41±0.20
83	1.69±0.65	1.87±0.36	1.48±0.36	0.73±0.24	0.78±0.07	0.69±0.15

Extracellular enzyme activities

Leu-aminopeptidase (LEU) activity increased from the beginning of the experiment, and the highest values were depicted on day 83 (Fig. 2.3). In contrast, phosphatase PHO activity increased slowly until day 21 and was maintained until the end of the experiment (Fig. 2.3). At the end of the experiment, PHO activity was the highest, followed by LEU and β-glucosidase (BG) activities. Significant increases in phosphatase activity were observed at day 83, significantly at the bottom of the tank. BG was significantly higher in surface sediment and decreased with increasing depth for the whole experiment.

Differences in extracellular enzyme activities were observed under different oxygenic conditions. PHO and LEU activities significantly reduced in anoxic conditions, compared to oxic conditions (up to 82% in the former). In contrast, BG activity was not significantly affected by oxygen concentrations. The ratio between degradation of organic matter containing carbon and nitrogen (BG:LEU) measured under oxic conditions showed a slope of 0.90, close to the equilibrium value between the enzymes (Fig. 2.4). In contrast, slopes for ratios of BG:PHO and LEU:PHO were 0.56 and 0.54, respectively, indicating enhanced ability to degrade organic compounds containing phosphorus.
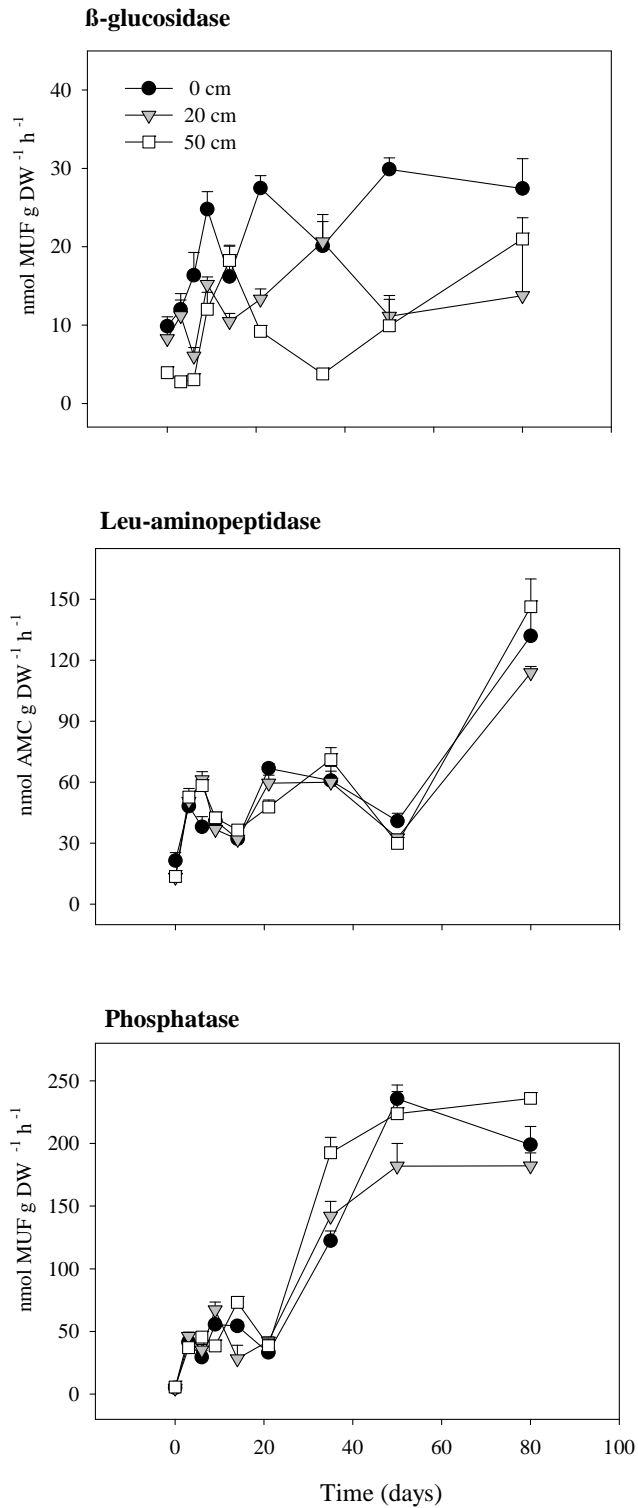
ß-glucosidase

Leu-aminopeptidase

Phosphatase

Figure 2.3. Temporal changes in extracellular enzymatic activities at 3 different depths. Values presented display mean ± standard error (from 3 replicates).
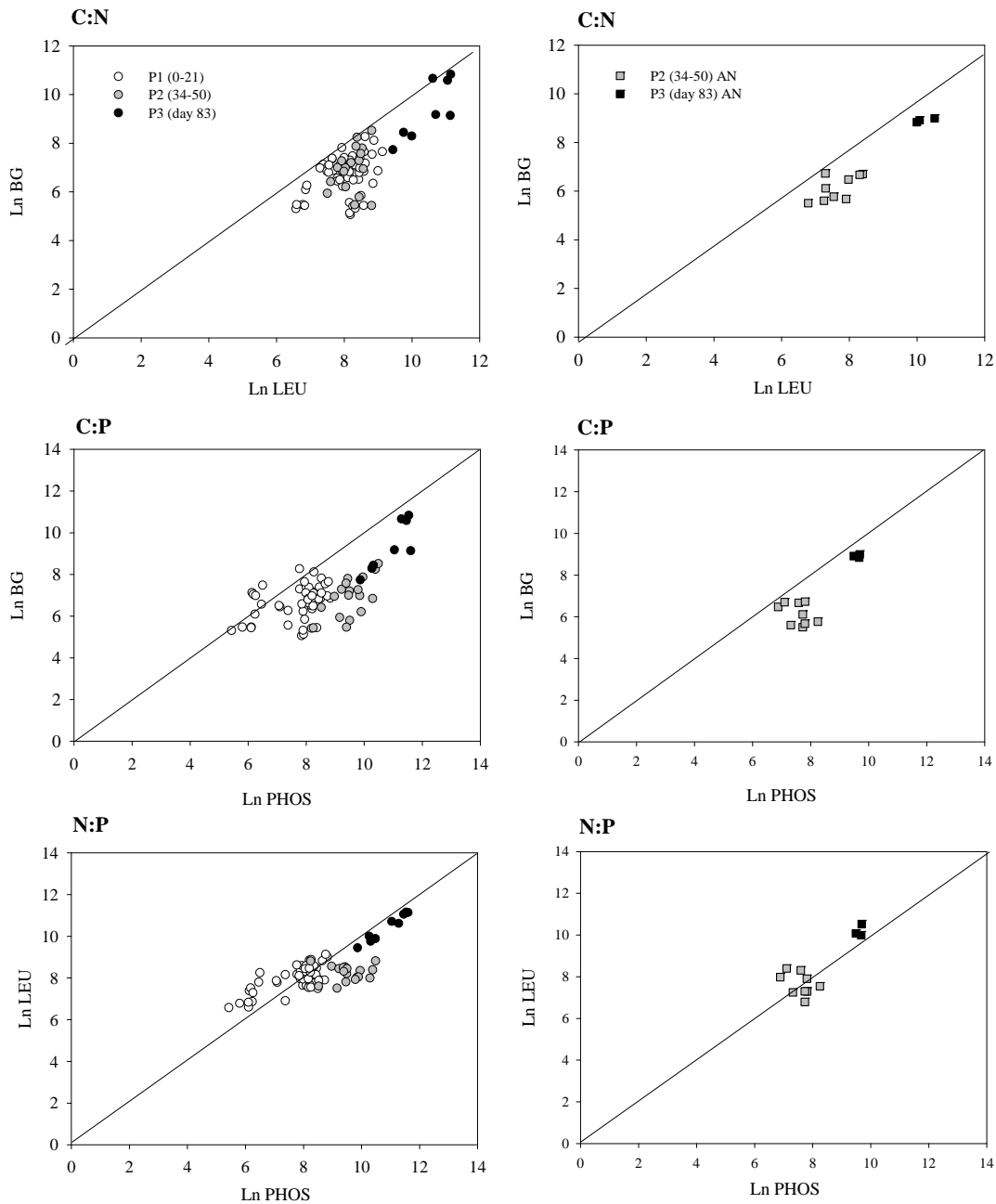
Figure 2.4. Relationships (in log space) between β-Glucosidase and peptidase (a) β-Glucosidase and phosphates (b), and peptidase and phosphatase (c) organic matter acquisition. Data are values from each sampling data and grouped by periods (P1 white, P2 grey and P3 dark). Anoxic ratios are also added on the right- The solid line indicates a 1:1 relationship.

The largest increase in PHO relative to BG and LEU was observed during P3, indicating that microbial communities first acquired more C and N, while P was

mostly assimilated by the end of the experiment (Fig. 2.4). Slopes close to 1 were measured in anoxic conditions at a depth of 50 cm. No differences in ratios of extracellular enzyme activities with depth were observed (data not shown).

Carbon substrate utilization profiles

Biolog Ecoplates were used to characterize the functional diversity and metabolic fingerprint of the sediment column communities according to depth and time (Fig. 2.5). The percentage of positive wells ranged between 65 - 100%, with lowest values being measured at the end of the experiment. Consistently, functional diversity (Shannon index) and functional richness (positive wells) also decreased significantly with time. Significant differences were found at different sediment depths; functional richness was highest at the surface and decreased with depth over time (see also Table 3). However, at 50 cm, measurements under oxic and anoxic conditions were not significantly different in statistical terms. Moreover, differences in the use of nitrogen compounds (NUSE index) at different depths were detected; high values were found at 50 cm on day 83.

The change in the metabolic fingerprint with depth was also remarkable. The community present at depth 50 cm was clearly distinct from that of the surface and the first 20 cm, as shown in the NMDS plot (Fig. 2.6a) and in the ANOSIM analysis. At 50 cm, microbial communities were able to degrade amino acids and carboxylic acids, including L-asparagine and pyruvic acid, whereas surface and 20 cm communities principally degraded polymers (Tween 80) and carbohydrates (α-D-lactose and D-xylose) (Fig. 2.6a). At 50 cm, high dispersion in the ordination analysis (NMDS) was found, indicating larger heterogeneity between samples (especially relevant on day 83).

Metabolic fingerprints of oxic and anoxic communities at 50 cm were different (Fig. 2.6b). However, anoxic samples from day 14 were similar to oxic samples from days 14, 34, and 50, whereas day 83 samples were not similar under oxic and anoxic conditions (Fig. 2.6b). Under anoxic conditions, decomposition of

carboxylic acids and amino acids were enhanced, whereas phenolic compounds and amines were degraded in the presence of oxygen.
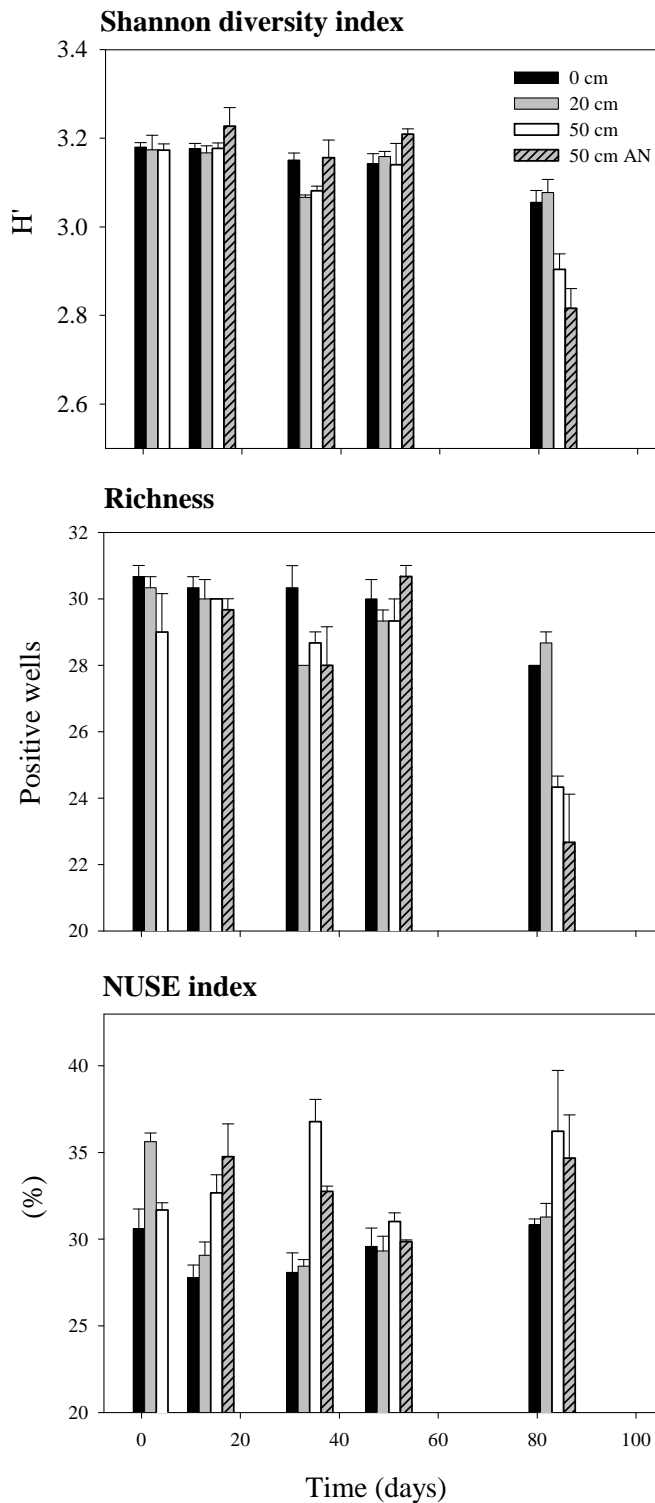
Figure 2.5. Shannon diversity, Richness (positive wells) and NUSE indices at depths 0,20 and 50 cm, for 5 different sampling dates. Values at 50 cm in anaerobic incubations are also

included after day 14. Values displayed include means and standard deviations (from 3 replicates).

Figure 2.6. NMDS ordination plots based on Bray-Curtis distances according of 31 substrates of Biolog Ecoplates after 144 hours of incubation. a) Data include all depths, colour indicates different depths and numbers the sampling date; b) Data separating only the 50 cm depth

values after different oxygen incubations conditions, Colour indicates oxic/anoxic incubated samples, and numbers the sampling date. The six groups of carbon substrates are fitted on the ordination plot $p < 0.05$. Kruskal 2D stress is equal to 0.15 and 0.11 respectively.
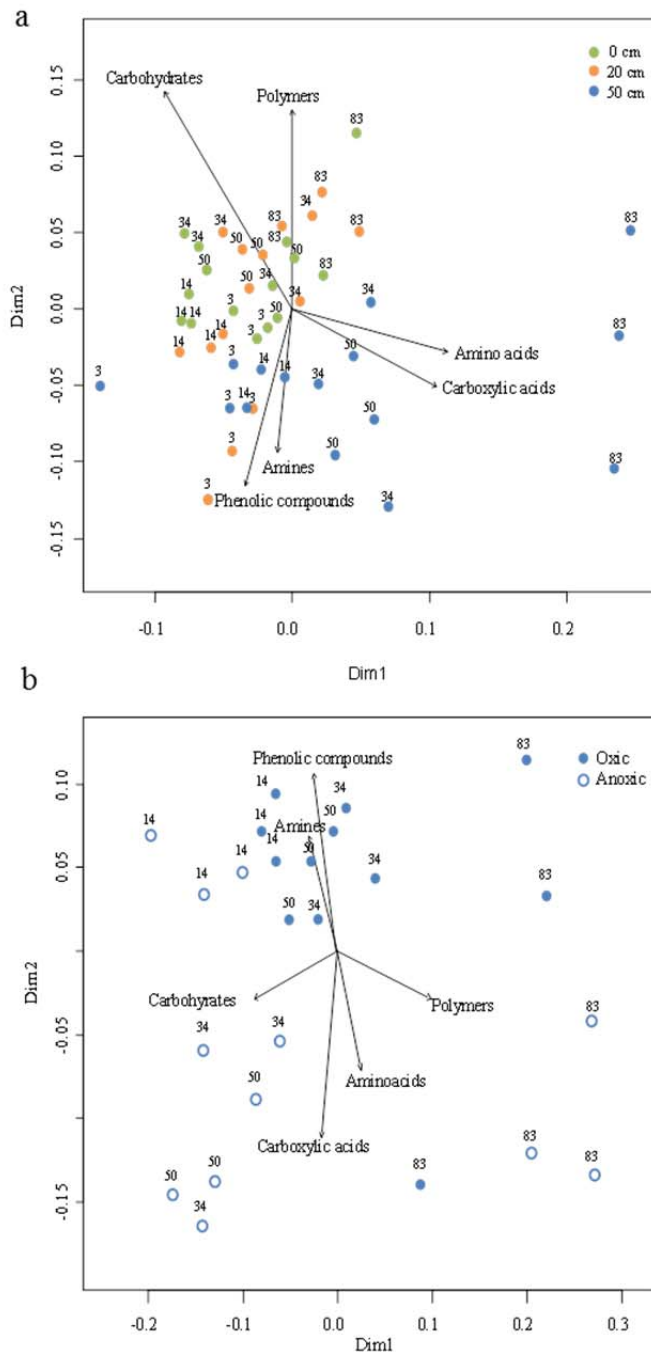
Average Well Colour Development (AWCD) values revealed significant differences in the kinetic parameters *a* and *x0* between oxic and anoxic incubation conditions at 50 cm. Under aerobic conditions, metabolic activity took longer (higher *x0* values) to achieve maximum colour development and higher maximum metabolic capacity (*a*) was observed on all sampling dates. In contrast, no differences were observed between oxic and anoxic conditions at day 83.

2.4 Discussion and relevance of the experimental work

Changes in microbial metabolism and functional diversity with depth were found to occur in a controlled porous media subject to continuous infiltration. To complement previous studies describing the structure and activity of microbial communities driven by physicochemical factors (e.g., water content, grain size, oxygen, pH, temperature, and redox potential), we report changes in microbial metabolism as a function of sediment depth and oxygen conditions.

Our findings indicated that bacteria colonizing the sediment column had different capacities to decompose organic compounds, depending on depth. At the surface, bacteria used simple polysaccharides through β-glucosidase activity, which decreased with depth. Previous studies documented also the decrease of β-glucosidase activity in a sand filter (Hendel et al., 2001) and deep-sea sediments (Boetius et al., 2000), although other studies linked decreased polysaccharide activities in deeper sediment to reduced availability or low bacterial density (Fischer et al., 2002). We found no significant differences in alive or total bacteria density. Also, environmental factors (pH, temperature, oxygen, and nutrient availability) in the upper soil layers are responsible for the reduced enzyme activities that occur with increasing depth

(Douterelo et al., 2011). However, no significant differences in temperature or pH were observed during the experiment.

Although significant oxygen content deplete was measured, the decrease in β-glucosidase activity with depth could not be explained by low oxygen content, as the activity was not affected by incubation with different oxygen conditions (Fig. 2.4). According to Kristensen et al. (1995), the availability of labile organic matter limits bacterial heterotrophic activity in aquatic ecosystems, regardless of oxygen concentration. Therefore, the decrease in simple polysaccharide use with depth may be explained by the accumulation of labile material at the tank surface and more resistant material in deeper sediments. We did not observe a difference in DOC with depth despite the high infiltration rates measured.

However, degradation of organic compounds containing nitrogen and phosphorus remained approximately constant with depth (Fig. 2.3). This may be due to bacterial colonization as indicated before, but also to the availability of organic N and P compounds at different depths. The delayed increase in phosphatase activity may indicate that few (if any) complex- P-compounds were present at the beginning of the experiment, and that bacteria may be producing complex P-compounds during the experiment.

Microbial functional diversity was also depth dependent, and differences were more evident by the end of the experiment. Biolog Ecoplates incubations were used to characterize carbon source utilization in the sediment tank. By the end of the experiment, the microbial community had become more specialized and used a narrower range of carbon substrates, as indicated by the lower Shannon diversity and richness scores. These data suggested that the microorganisms had assembled to those better adapted to the environmental conditions of the sediment column. Decreased use of available substrates was observed at 50 cm, similar to results reported by Griffiths et al. (2003), who showed decreased substrate utilization in the surface soil at 20 cm.

The microbial community also showed different fingerprints depending on depth (Fig. 2.6). Carbohydrates and polymers were used readily at the surface (0 and 20 cm). These compounds are considered to be the largest bioavailable source

of carbon in sediments (Oliveira et al., 2010) and greater use of them at the surface is consistent with high surface β-glucosidase activity. The metabolic fingerprint at 50 cm was distinct from fingerprints at 0 and 20 cm; the former was mainly characterized by the use of nitrogen compounds (higher NUSE index values). Until day 50, microbial communities used amines and phenolic compounds and from day 50 until the end of the experiment, amino acids and carboxylic acids were used. These results indicate the significant use of nitrogen-containing organic compounds at the bottom of the tank, consistent with the maintenance of leu-aminopeptidase activity.

Differences in microbial metabolism with depth may have been affected by oxygen availability, most significantly by the end of the experiment. Bacterial colonization and biofilm formation may have contributed to pore clogging, providing a substantial decrease in permeability and infiltration flow rate, and an increase in anoxia with increasing depth. Indeed, oxygen plays an important role in microbial metabolism and diversity (Brune et al., 2000). In our study, a significant reduction of degradation of organic nitrogen and phosphorus compounds was found under anoxic conditions, whereas no polysaccharide degradation was detected (Fig. 2.4), suggesting that inactivation rates of the hydrolytic enzymes vary for different enzymes.

Christy et al. (2014) reported that during anaerobic and aerobic decomposition, polysaccharides are hydrolysed by secreted enzymes, such as cellulase and cellobiase. Cellulose-hydrolysing enzymes, including β-glucosidase, can be released under different oxygen conditions. In contrast, hydrolysis of organic phosphorus compounds was inhibited by anoxic conditions. The differential effects of anoxia on extracellular enzyme activities at different depths affected the balance C:N:P. In the experiment, oxic conditions led to greater degradation of phosphorus compounds compared to carbon and nitrogen over time. Equilibrium was observed between C:N acquiring enzymes, but it remained imbalanced for C:P and N:P acquiring enzymes (Fig. 2.4). These data suggested that the sediment community inside the tank was phosphorus limited, especially at the end of the experiment.

Phosphorus limitation in sediment affects bacterial growth rates and microbial nutrient assimilation; however, due to inhibition of phosphatase activity under anoxic conditions, the equilibrium between phosphorus-acquiring enzymes and carbon- and nitrogen-acquiring enzymes was re-established (Fig. 2.4).

The significant depth effects observed at the end of the time-course and the effect of anoxia were shown in the functional fingerprint measured at 50 cm (Fig. 2.6b). A different functional fingerprint was obtained for communities incubated in oxic and anoxic conditions; carboxylic acids and amino acids were used preferentially under anoxic conditions. The distinct metabolic fingerprints occurred gradually over time; e.g., results for day 14 in anoxia were still similar to those found under oxic conditions. The gradual change in oxygen conditions that occurred in the column suggests that both aerobic and anaerobic processes may have occurred simultaneously. Indeed, nitrification and denitrification processes might also have occurred with time, as shown by NH_4^+ consumption and NO_3^- production in the first 20 cm of the column. Toward the bottom of the tank, NO_3^- was consumed and no ammonium was present, suggesting that nitrogen had to be acquired from complex nitrogen compounds. These data hint the spatially coexistence of nitrification and denitrification in the sediment profile, already reported in marine sediments (Bonin et al., 1998).

The gradual change in the metabolic fingerprint with increasing depth may be related to changes in the available OM and in the metabolic processes that occur due to depleted oxygen concentrations. However, changes in the composition of bacterial communities through the column may also occur. Adaptation of the communities to anoxic conditions was shown by the presence of active bacteria at all depths. Facultative bacteria, adapted to live in sediments with changeable oxygen concentrations, may have colonized the column. Indeed, microorganisms responsible for oxidation of organic matter are not only aerobic bacteria; in hypoxic areas, components of anaerobic respiration (nitrifiers, sulphate reducers, and methanogenic bacteria) can metabolize organic carbon (Kristensen et al., 1995). The data indicated that aerobic and anaerobic communities metabolized substrates in the plate with similar

velocities, suggesting that the microbial communities adapted to the environmental conditions after the lag phase.

Our experiments revealed higher heterogeneity between replicates at greater depths and under anoxic conditions, especially at the end of the experiment, indicating larger spatial heterogeneity combined with lower functional richness and diversity. Functional heterogeneity may be linked to physicochemical conditions in sediments, which appear to have high spatial and temporal heterogeneity at greater depths. Complementary information on the microbial community in the sediment column was provided by extracellular enzyme activities and Biolog Ecoplate incubations. The former reflect the inherent activity of the resident community, whereas the latter assess the potential functional diversity of microbial communities. In our study, extracellular enzyme activities showed larger differences over time compared to Biolog Ecoplates, which were more sensitive to spatial differences. Altogether, this indicated that the biogeochemical processes changed over time, whereas the functional diversity characteristics changed due to sediment depth.

The laboratory experiments used simulated natural sediment conditions and allowed the environmental conditions to be controlled, enabling a meso-scale study. Extrapolation of these results to full-size MAR facilities must be done with caution, and the transferability of these results at larges scales should be assured through field experiments.

3 Fate of EOC's in groundwater: conceptualizing and modelling metabolite formation under different redox conditions

3.1 Introduction

The presence of pharmaceutical compounds in aquatic environments has been frequently addressed in recent years, and it is the topic of numerous review articles (Gavrilescu et al. 2015, Schwarzenbach et al. 2006). The discharge of antibiotics into the environment has become a major concern, as this group of pharmaceuticals is prone to directly influencing microbial communities. Antibiotics may enter the environmental system via wastewater or else as wastewater treatment plant (WWTP) effluents, diffusive agricultural input, or landfill discharge, and they can be found in all environmental compartments, from surface and subsurface water bodies, to sediments and soils.

Sulfamethoxazole (SMX) is a polar sulphonamide antibiotic, and the most widely detected antibiotic in aquatic environments (Gao et al. 2014). SMX mainly enters wastewater via human excretion, either unmodified, or as its human-metabolized transformation products, N-acetyl-SMX or N-SMX-glucuronide (Göbel et al. 2005). Both transformation products are easily cleaved back to the SMX parent compound. Since SMX is not completely degraded in wastewater treatment plants (Kümmerer, 2009), it is found in minute concentrations in the WWTP water effluents, eventually reaching soils and surface or subsurface water bodies. SMX has a very low adsorptivity to most soils (Schaffer et al. 2015). In general, the literature on SMX degradation in both WWTPs and natural aqueous environments is marked by inconsistent results. This is supposedly because elimination amounts and rates depend on various environmental factors such as in situ redox potential, available nutrients, soil characteristics, seasonal temperature, microbial adaptation, and light variations (Müller et al. 2013), all such factors being site-dependent and temporally variable.

Based on field observations and laboratory experiments, it is postulated that degradation of SMX is biologically mediated and occurs preferentially under

anaerobic conditions (e.g., Schaffer et al. 2015). Some lab experiments reported the fate of SMX for particular redox conditions such as denitrification (Barbieri et al. 2012, Nödler et al. 2012) or iron reducing conditions (Mohatt et al., 2011). Nevertheless, aerobic degradation of SMX has also been observed in aerobic environments such as activated sludge (e.g., Reis et al. 2014). Only in experiments performed under either aerobic conditions (Reis et al. 2014), or in anaerobic iron reducing conditions (Mohatt et al. 2011), the irreversible breakage of the SMX molecule was observed. Contrarily, the metabolites observed during denitrification conditions resulted from the substitution of the primary amine of SMX, forming either 4-nitro-SMX or else desamino-SMX (Barbieri et al. 2012, Nödler et al. 2012). In these last two papers, the authors reported that metabolites were not stable, meaning that when the denitrification process was over they were retransformed into the parent compound.

Despite the existing literature dealing with the fate of SMX under different redox conditions, there is little work postulating the processes taking place at the molecular scale, proposing closed-form expression for reaction rates, and reproducing the experimental observations of SMX fate through mathematical modelling. Most published work assumes that degradation can be explained by (apparent) first-order degradation rates for all EOCs; only few studies have investigated quantitatively the actual processes driven by varying redox conditions over degradation rates of EOCs (e.g., Liu et al. 2013). Moreover, this simplified approach, based on first-order reactions, accounts only for the presence of irreversible reactions, contradicting a number of experiments where reversibility of the transformation processes has been observed. While it is obvious that each antibiotic displays an individual, non-generalizable degradation behaviour, we believe that understanding one of them will open the door to analyse in the future the fate of a cocktail of antibiotics (and their metabolites), including also potential synergies.

The objective of this work was to develop a conceptualization of the molecular mechanisms of degradation of the SMX molecule under different redox conditions ranging from aerobic to iron-reducing conditions, and a mathematical model capable of reproducing these mechanisms, with the overall aim of tracing

the metabolite formation from different degradation pathways. To illustrate the conceptual and mathematical work, we model and interpret three published experiments, two of them performed under nitrate reducing conditions (Barbieri et al., 2012; Nödler et al., 2012), and one under iron reducing (Mohatt et al., 2011).

3.2 Methods

3.2.1. Observations and conceptualization of the molecular mechanisms

The literature provides information regarding degradation of SMX only under aerobic and partially under anaerobic (nitrate and iron reduction) conditions states. Although in Mohatt et al. (2011) SMX degradation under sulphate reduction condition was observed, no experimental information is available describing such process, and thus no metabolites have been observed. So, in this work we conceptualize the SMX degradation for aerobic conditions, denitrification, and iron reducing conditions.

3.2.2. SMX behaviour under aerobic conditions

Aerobic degradation of SMX has been mostly studied in the context of WWTPs and surface water bodies, and it is not expected to be a significant process in groundwater bodies due to their generally low oxygen concentrations. Degradation has mostly been observed for large SMX concentrations and with acclimated biomass in active sludge systems. SMX degradation was observed either via direct metabolism or via co-metabolism (Reis et al., 2014; Drillia et al., 2005); in the latter case, degradation rates were generally comparably larger. Additionally, one study reported aerobic degradation of SMX in a column experiment supplied with surface water (Baumgarten et al. 2011). The degradation was linked to large adaptation times, around 1 year for the

degradation at the lowest concentration of SMX (0.25 µg/L) and 3-12 months for the highest reported one (1.4 µg/L).

The most frequent metabolite produced under aerobic conditions is 3-amino-5-methylisoxazole (Reis et al. 2014). This metabolite represents an irreversible breakage of the SMX molecule, more precisely of the sulphonamide radical (Figure 3.1). This pathway would facilitate the complete mineralization of 4-aminobenzolsulfonate (a by-product of the reaction), as this compound could also be degraded under aerobic conditions (Gao et al. 2010).
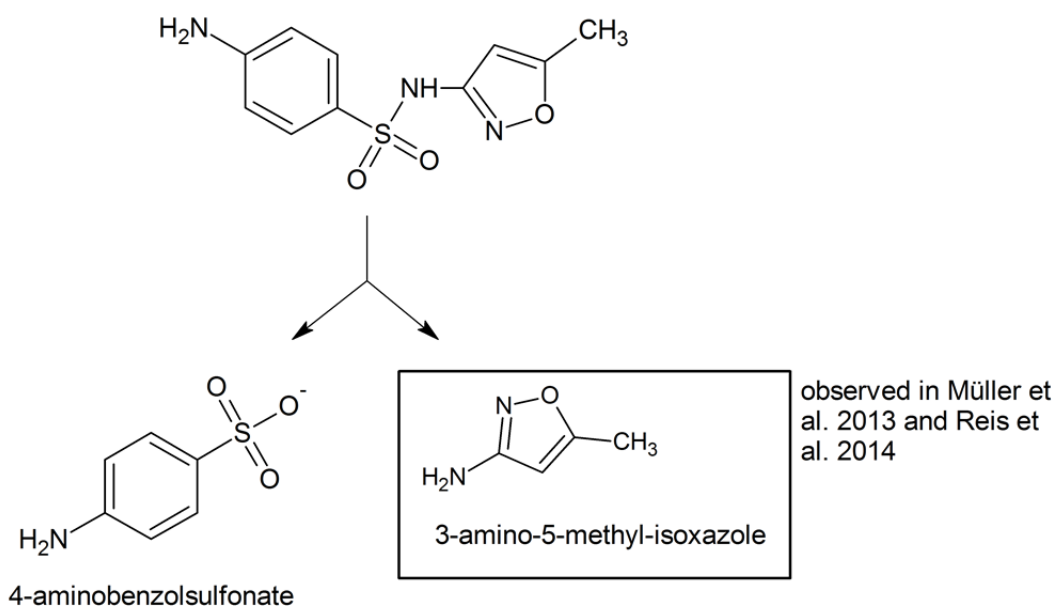
Figure 3.1. Pathway of aerobic degradation of SMX proposed by Gao et al. (2010) and later confirmed experimentally by Müller et al. (2013) and Reis et al. (2014).

Several authors state that aerobic degradation can be modelled as first-order kinetics, based on an apparent half-live parameter. Reported half-live values in the literature were determined whenever biomass was completely acclimated; this would indicate that in more general systems, with no acclimated biomass, real half-lives (if at all existing) would be larger.

3.2.3. SMX behaviour under nitrate reducing conditions

SMX degradation under nitrate reducing conditions has been widely reported (Banzhaf et al. 2012, Barbieri et al. 2012, Nödler et al. 2012). Because of the controlled conditions of the experiments and metabolite monitoring we have focused our analysis in the works of Barbieri et al., 2012 (from now on BAR) and Nödler et al., 2012 (denoted NDL in the sequel).

Observations and process inference

The BAR and NDL experiments were developed under identical experimental conditions, involving sets of microcosms containing natural sediments, synthetic water and SMX (injected in a EOCs cocktail). They included a set of biotic and abiotic series by duplicate to separate biodegradation (both biotic mineralization and transformation included) from sorption. The experiments were performed inside a glove box under Argon atmosphere and into 0.3 L glass bottles running for 21 days in the BAR experiment and 90 days for NDL. Bottles were filled with 0.24 L of water with the chemical signature provided in Table 3.2 and 120 g of air-dried and homogenized quaternary alluvial sediments. The organic carbon and the nitrogen present in the sediment were lower than 0.2% in mass. Mn and Fe (III) associated to oxide-hydroxides and oxides were 0.007% for Mn and 0.584% for total Iron. Denitrification conditions were stimulated by adding easily degradable organic compounds (sodium acetate and methanol) to act as electron donors. Analytical details can be found in Barbieri et al. (2012). Concurrently, a set of abiotic experiments were performed with an identical setup except that a small concentration of $HgCl_2$ was added to the solution in order to inhibit biological activity.

The results of the biotic experiments showed a decrease of nitrate and organic carbon with time after lag phases of 1.8 and 1.2 d in the BAR and NDL experiments, respectively (Figures 3.2a and 3.2d). The lag phase was attributed to denitrifying bacteria adaption period. A transient accumulation of nitrite, simultaneous with a decrease in nitrate was observed. After 10 days, nitrate and nitrite were completely depleted in the BAR experiment, indicating complete denitrification, and a small production of Mn^{+2} and Fe^{+2} was observed indicating

a transition towards stronger reducing conditions. Instead, in the NDL experiment, denitrification was active after 90 days, with remaining concentrations of nitrate and nitrite of 3.5 and 0.16 mM, respectively, suggesting incomplete denitrification by the end of the experiment.
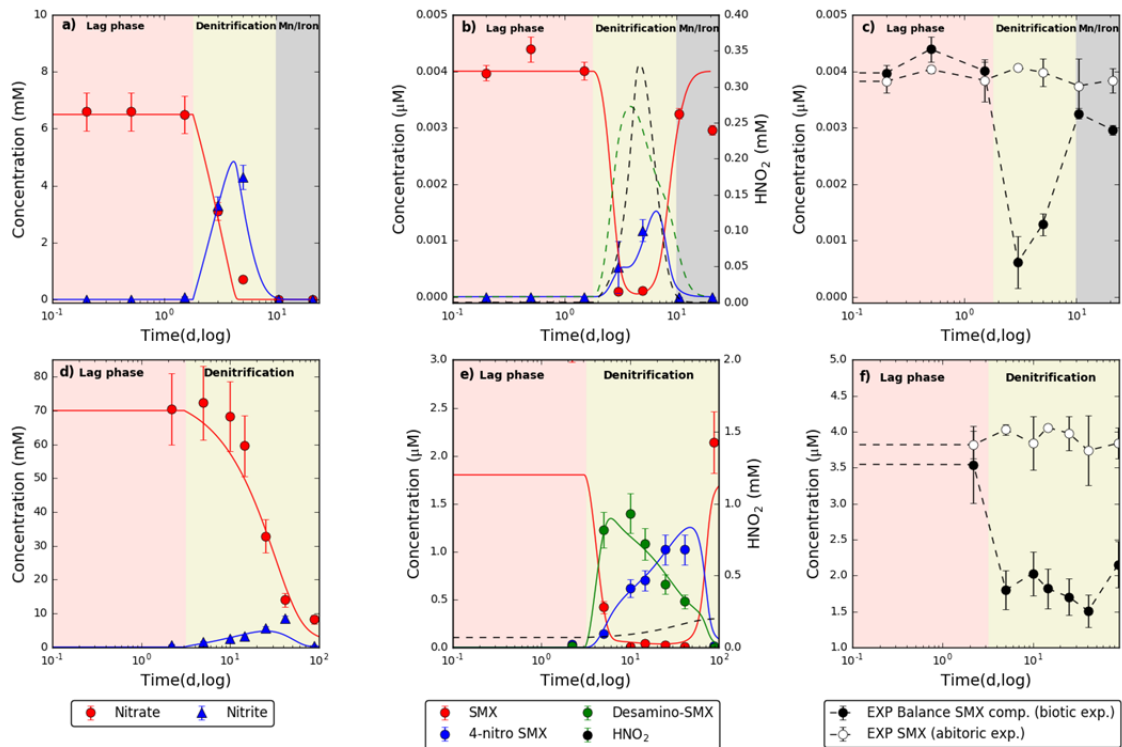

Figure 3.2. Experimental information of Babieri et al. (2012) (a, b, c) and Nödler et al. (2012) (d, e, f) (points) and modelled results of nitrate and nitrite (a,d), sulfamethoxazole, 4-nitro sulfamethoxazole, desamino-sulfamethoxazole and nitrous acid (b,d). The time axis is displayed in log scale. The extremes of the bars associated with each individual measurement indicate the values obtained from two replicates, while dots display their arithmetic average. Solid lines represent the results from the modelling effort (Section 3.1). Dashed lines in b) and e) represent expected (from the model) concentrations of non-measured elements.

Almost full depletion of SMX was observed during the period corresponding to transient accumulation of nitrite in both experiments (Figures 3.2b, 3.2e). During this time, 4-nitro-SMX was detected and quantified in both experiments, whereas a second metabolite, desamino-SMX, was also detected in NDL

experiment (not monitored in BAR). After denitrification was over (BAR) or close to being complete (NDL), the two metabolites were virtually depleted in the system, while SMX reappeared, reaching concentration values of the same order than the initial injected ones. At this point it is relevant to state that the NDL experiment involved an initial concentration of SMX 1000 times larger than that of BAR (see Table 3.1), indicating that the process was not an artefact attributable to high or low input concentrations.

Table 3.1. Hydrochemistry of the input water used in the BAR and NDL experiments.

	Barbieri et al. (2012) experiment (BAR)	Nödler et al. (2012) experiment (NDL)
SMX (µM)	0.004	4
Nitrate (mM)	6.7	67.7
Organic carbon (mM)	9.7	71.5
Alkalinity (mM)	1.0	0.7
Calcium (mM)	2.9	3.1
Sodium (mM)	9.1	11.1
Potassium (mM)	1.0	1.2
Sulfate (mM)	2.0	1.9
Iron (Fe^{+3}) (mM)	0.001	0.001
Manganese (Mn^{+4}) (mM)	0.001	0.001
pH	8.5	7.3
Temperature (ºC)	25	25

Regarding the abiotic experiments, no denitrification was observed at any sampling time, and the concentration of SMX remained constant during all the duration of the experiment indicating that SMX depletion in the biotic experiments was driven by biological activity (Figures 3.2a-f).

Concerning the mass balance of SMX compounds, the BAR experiment showed a gap during the denitrification phase, and by the end of the experiment the concentration of SMX was about 75% of the initial value (Figure 3.2c). On the other hand, the mass balance in NDL had a sudden decay of about 45% at the first sampling point (day 5) and from then on it remained approximately constant until the end (day 90) of the experiment (Figure 3.2f). As experimental conditions were similar in the two experiments, we assumed that the gap observed in the mass balance of BAR could represent the formation of the

desamino-SMX metabolite (not measured). Thus, it seemed that a part of SMX disappeared in an unknown pathway when denitrification started (18 ± 6% and 45 ± 2% in the BAR and NDL experiments, respectively), whereas the remainder was fully transformed into 4-nitro-SMX and desamino-SMX. These two metabolites were unstable and re-transformed into SMX, the parent compound, when nitrate and nitrite were (almost completely) depleted.

Conceptualization

The generation of the two metabolites 4-nitro-SMX and desamino-SMX in the BAR experiment was ascribed to the denitrification activity enhanced by the presence of a large external source of organic carbon. In both metabolites the key point is the substitution of the primary amine of sulfamethoxazole by different radicals. The formation of 4-nitro-SMX implies the nitrosation of the primary amine of SMX, whereas desamino-SMX involves the deamination process again of the primary amine. From these considerations, we propose the conceptual model summarized in Figure 3.3.
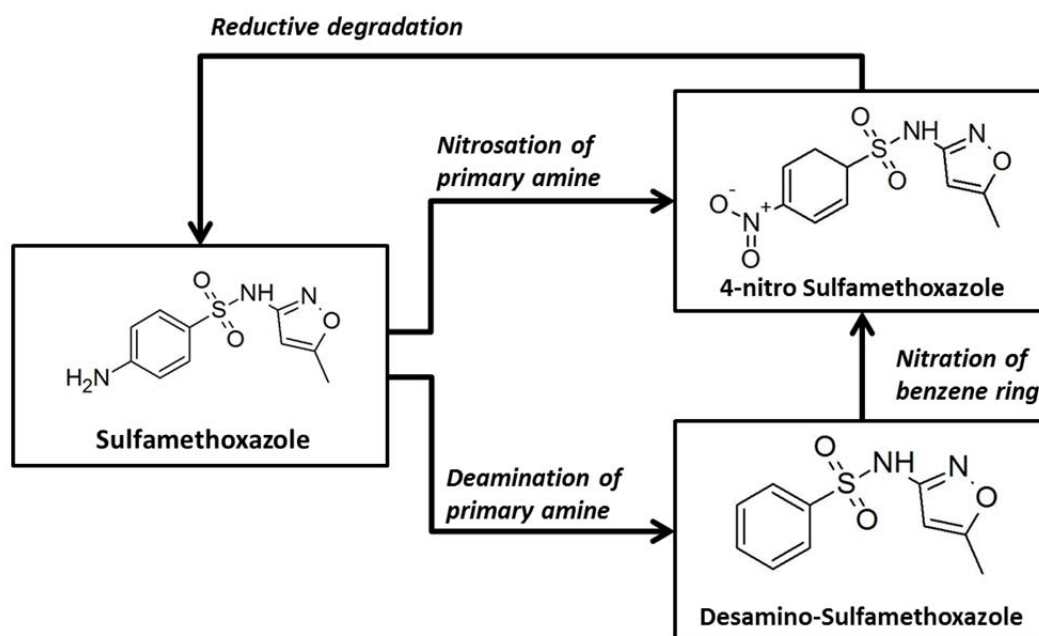

Figure 3.3. Conceptual model of processes involved in the fate of SMX under denitrifying conditions (italic letters) and the corresponding metabolites.

The occurrence of either nitrosation or deamination of the primary amine could be attributed to the presence of nitrous acid, the conjugate (weak) acid of nitrite (with pKa = 3.15 at 25ºC). The presence of nitrous acid facilitated the formation of a diazonium cation replacing the amine radical in SMX. This compound was not stable under ambient conditions and could undergo numerous consecutive fast reactions, strongly depending on reaction conditions and available reaction partners (Carey and Sundberg 2007). One reaction path implies diazonium reacting again with another acid nitrous molecule forming 4-nitro-SMX. A second path implied the reaction of the diazonium molecule with an alcohol (methanol was present in the experiment), forming a desamino-SMX molecule.

Note that the formation of 4-nitro-SMX and desamino-SMX were both driven by the presence of HNO2, a subproduct of the denitrification process. Nonetheless, the reaction of degradation of SMX was abiotic, meaning that SMX did not participate in the denitrifying metabolism. Thus, the co-metabolic pathway of degradation consisted in the generation of nitrite as an intermediate product of denitrification. At that point, nitrite was conjugated with HNO2, responsible to generate an abiotic reaction with a diazonium salt as an intermediate product, and the last responsible of the observed decay of SMX concentrations.

The retransformation of 4-nitro-SMX into SMX was confirmed by Nödler et al. (2012), which proved the reduction of 4-nitro-SMX to its corresponding amino-compound (SMX) in the absence of denitrification. The molecular mechanism proposed is reductive degradation, similar to the degradation of nitrobenze to aniline, involving an overall inclusion of 6H+ and the removal of 2H2O molecules. The reductive degradation could be mediated biotically or abiotically, with no information available to allow discriminating between them.

Concerning the fate of desamino-SMX and the mass balance in the NDL experiment, it seemed logical to infer that it was also retransformed into SMX. The most common mechanism for the reintroduction of nitrogen functionality into aromatic rings (in form of nitro radical) is nitration, which would imply creating a nitro-aromatic compound, here again 4-nitro-SMX. After that, the nitro compound could be reduced easily to the corresponding amino derivatives. The

active nitrating species would be the nitronium ion, NO_2^+, which would be formed by the protonation and dissociation of nitric acid in the presence of sulfuric acid, acting as a catalyst.

To sum up, the complete conceptual model of SMX under denitrifying conditions would imply the formation of two metabolites (4-nitro-SMX and desamino-SMX), which are not stable and are retransformed to the parent compound, directly in the case of 4-nitro-SMX or with a previous transformation to nitro compound for desamino-SMX. The full reaction chain is summarized in Figure 3.3.

3.2.4. SMX behaviour under Fe reducing conditions

Degradation of SMX under iron reducing conditions was described in Mohatt et al. (2011) based on experimental work. The authors proposed a process based on the electron flow produced by the re-oxidation of ferrous iron (II) to ferric iron (III) taking place on the surface of goethite, which facilitates the break of the SMX molecule. As Fe(II) was previously produced by biological reduction of Fe(III), the degradation of SMX occurred, again, as a result of a co-metabolism process initiated by labile organic carbon degradation.

The conceptualization of degradation processes under iron reducing conditions is summarized in Figure 3.4. The metabolite formed is the result of the breakage of the isoxazole ring, so that four metabolites can be formed (Table 3.2), each one following a particular degradation pathway (Mohatt et al. 2011).

Table 3.2. Metabolites of SMX detected during iron reducing conditions
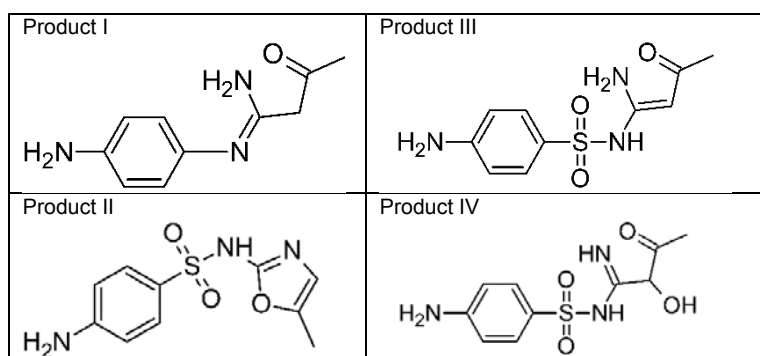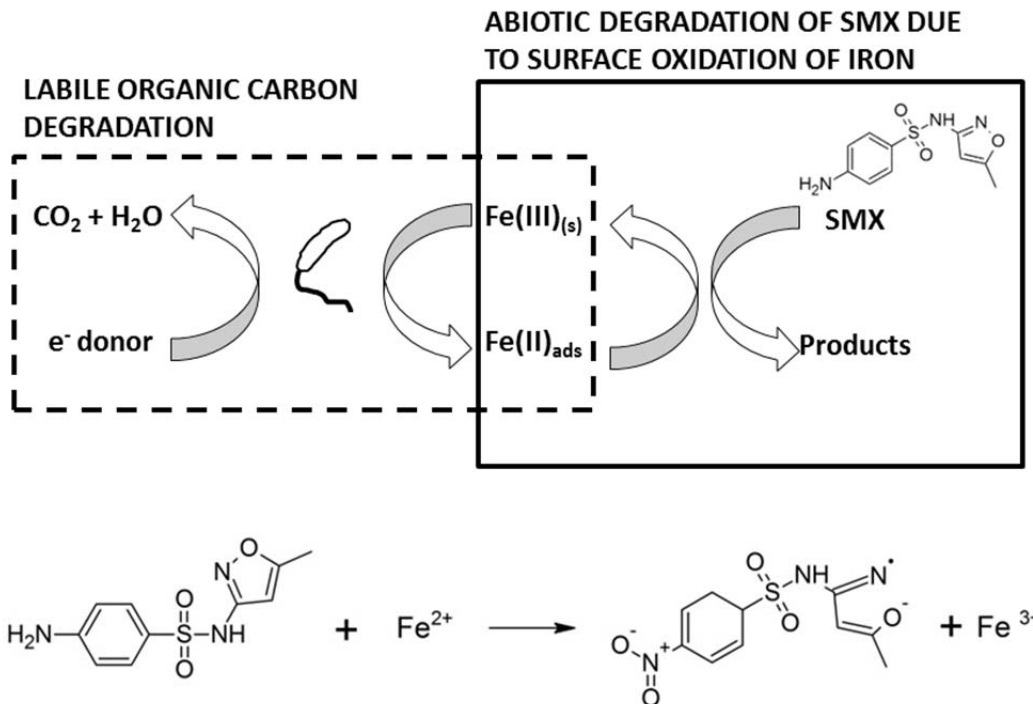
Figure 3.4. Conceptual model of SMX due to the abiotic oxidation of iron due to a previous reduction of goethite biologically mediated (modified from Mohatt et al. (2011)).

Note that depending on the existing redox state, the metabolites generated are very different. Whereas during denitrification the metabolites formed involve the reversible substitution of the amine radical, during either aerobic or iron reduction conditions the isoxazole ring is irreversibly broken, thus facilitating the eventual mineralization of SMX.

3.3 Model Development

Coupling denitrification model with SMX degradation and metabolite formation

As indicated by the conceptual model, we postulated that the key abiotic process controlling SMX degradation in the experiments was the presence of

nitrous acid linked to nitrite accumulation. The first step in the modelling process consisted in developing a biodenitrification model capable of accounting for the transient accumulation of nitrite, and its subsequent equilibrium with nitrous acid. The model considered a multiple-Monod expression incorporating two terms: one for the electron donor (organic carbon) and another one for the electron acceptor, plus two reduction steps: (1) nitrate to nitrite, and (2) nitrite to dinitrogen gas (see the matrix of rates and components in Table 3.3). The general Monod expression was defined as:

$$r = K_{max} \frac{[ED]}{[ED]+k_{s,ED}} \frac{[EA]}{[EA]+k_{s,EA}} \frac{k_I}{[I]+k_I} [X] \qquad (1)$$

where [ED] is the concentration (ML^{-3}) of the electron donor (organic carbon). [EA] that of the electron acceptor (nitrate or nitrite, ML^{-3}), and [X] the biomass concentration [ML^{-3}]. Yh (microbial yield) and Q are stoichiometric parameters [-]; kmax [T^{-1}] is the maximum consumption rate of electron donor; and Ks EA and Ks ED [ML^{-3}] are half-saturation constants. As the presence of nitrate limits the reduction of nitrite, an inhibition factor accounting for the presence of nitrate was added to the electron donor rate, with a constant k_i [ML^{-3}].

Table 3.3. Processes, components and rates involved during degradation of SMX under denitrifying conditions. The stoichiometric coefficients were determined from complete reactions.

Process	Components										
	C_{org}	C_{inorg}	NO_3^-	NO_2^-	N_2	H^+	HNO_2	HNO_3	SMX	4-NIT	DES
OM degradation due to nitrate reduction	-1	+1	-2.2	+2.2							
OM degradation due to nitrite reduction	-1	+1		-1.5	+0.75	+1.5					
Nitrite equilibrium with nitrous acid				-1		-1	+1				
Nitrosation of primary amine to 4-nitro-SMX							-2		-1	+1	
Nitrosation of primary amine to desamino-SMX	-1						-1		-1		+1
Reduction of 4-nitro-SMX to SMX									+1	-1	
Nitration of desamino-SMX to 4-nitro-SMX								-1		+1	-1

Process	Process rate
Organic matter degradation due to nitrate reduction	$K_{max} \dfrac{[C_{org}]}{[C_{org}] + k_{s,C_{org}}} \dfrac{[NO_3^-]}{[NO_3^-] + k_{s,NO_3^-}} [X]$
Organic matter degradation due to nitrite reduction	$K_{max'} \dfrac{[C_{org}]}{[C_{org}] + k_{s',C_{org}}} \dfrac{[NO_2^-]}{[NO_2^-] + k_{s,NO_2^-}} \dfrac{k_I}{[NO_3^-] + k_I} [X]$
Nitrite equilibrium with nitrous acid	$\dfrac{[NO_2^-][H^+]}{K_a}$
Nitrosation of primary amine and formation of 4-nitro-SMX	$k_1[SMX][HNO_2]^2$
Nitrosation of primary amine and formation of desamino-SMX	$k_2[SMX][HNO_2][C_{org}]P$
Reduction of 4-nitro-SMX and formation of SMX	$k_3[4-NIT]$
Nitration of benzene ring of desamino-SMX and formation of 4-nitro-SMX	$k_4[DES][HNO_3]$

The time evolution of denitrifying biomass was not measured. For simplification purposes, biomass was considered constant in time, but active only after a certain elapsed time (lag phase). The value was fixed to 1 mM, consistent with available models of denitrification in batch experiments (Rodríguez-Escales et al. 2014). The lag phases were 1.8 and 1.23 days corresponding to the period of inactive biomass for the BAR and NDL experiments, respectively. Nitrous acid concentrations were calculated considering its equilibrium with nitrite and a pKa of 3.15 (see Table 3.3).

The rate expressions of SMX metabolite formation were defined for each one of the processes conceptualized. The formation of 4-nitro-SMX was modelled as second-order with respect to nitrous acid (proportional to the square of the concentration) and as a first-order (linear) with respect to SMX, resulting in a global third-order expression. The reason of this expression is related to the stoichiometry of the reactions (see Figure 3.3 and Table 3.3). The formation of one mole of 4-nitro SMX requires two moles of nitrous acid, but only one mole of SMX. On the other hand, desamino-SMX formation was modelled as a third-order kinetic expression, being first-order with respect to the organic matter

(methanol), nitrous acid and SMX. The retransformation of 4-nitro-SMX into SMX was modelled as a first-order degradation with respect to the metabolite. Finally, the retransformation of desamino-SMX into the nitro compound was considered first-order with respect to the nitric acid and the metabolite, resulting in a second-order expression. Denoting the concentrations of sulfamethoxazole, 4-nitro-SMX and desamino-SMX respectively as [SMX], [4-NIT], and [DES], the corresponding driving equations read

$$\frac{d[4-NIT]}{dt} = k_1[SMX][HNO_2]^2 - k_3[4-NIT] + k_4[DES][HNO_3] \tag{2}$$

. $$\frac{d[DES]}{dt} = k_2[SMX][HNO_2][C_{org}]P - k_4[DES][HNO_3] \tag{3}$$

In (2) and (3), $[HNO_2]$, $[HNO_3]$, $[C_{org}]$, stand for nitrous acid, nitric acid, and labile organic carbon, respectively. The *k* parameters involved are degradation coefficients; *P* is the portion of methanol in the organic matter. Note that the rate of SMX would be equal to the sum of (2) and (3) with a change of sign.

Determination of parameters

The stoichiometric parameters of the model were determined (fixed) from the denitrification reactions (Table 3.3). The kinetic parameters were automatically calibrated using code PEST (Doherty 2005). Notice that this process involves two independent (not simultaneous) calibration processes. PEST code allowed computing the sensitivities, correlations, and linear uncertainties (confidence intervals) for the optimized model parameters using the Levenberg-Marquardt algorithm. The weights of each chemical species associated to the measurement errors were applied using the inverse of the standard deviation of the confidence interval of measurements (95%). For the calibration process, we used the experimental information (nitrate, nitrite, SMX, 4-nitro-SMX and desamino-SMX) provided by Barbieri et al. (2012) and Nödler et al. (2012). The initial concentrations of the model are summarized in Table 3.1.

Mathematical model and experiments of SMX under iron reducing conditions

The original model of SMX degradation under iron reducing conditions proposed by Mohatt et al. (2011) assumes an exponential decay for SMX,

focusing on a single abiotic degradation process. Our conceptual model is based on the reaction occurring on the surface of goethite, having a significantly different behaviour at early and at late times. At early times the exponential model fits properly the experimental data; this implies that the model is based on the availability of a large number of available sites for reaction at the goethite surface. Once these sites are mostly exhausted (intermediate to large times), additional ones must be found at deeper layers. The number of sites at those deep layers can be best modelled using a fractal approach, so that the reaction rate is best described by a power law. The governing equations are:

$$\frac{d[SMX]}{dt} = \begin{cases} -k_5[SMX] \\ -k_6[SMX]^n \end{cases} \tag{4}$$

where the k and n values are again degradation constants. The top expression in (4) is applicable for short times and the bottom one would be valid for intermediate to large times, with a transition of behaviour not clearly defined.

3.4 Results and Discussion

3.4.1. Fate of SMX under denitrifying and iron reducing conditions

Figure 3.2 displays the results of the modelling effort applied to the BAR (top row) and NDL (bottom) using the best-fitted parameters listed in Table 3.4. Figures 3.2a and 3.2d correspond to the biodenitrification process in terms of nitrate and nitrite concentrations. The corresponding inferred (not measured) presence of nitrous acid is displayed in Figures 3.2b and 3.2e. These same plots present the model fit of the concentrations of SMX and metabolites. SMX concentrations are reasonably well reproduced with the only exception of the last point in the BAR experiment; we associate this misfit to the model not accounting for Fe/Mn reduction conditions developing after 10 days. Regarding the concentration of 4-nitro-SMX, the model reproduced quantitatively the temporal behaviour in both experiments. Also, Desamino-SMX concentrations

were well reproduced for the NDL experiment (in the BAR experiment this value was only inferred, and plotted as a green dashed line).

Table 3.4. Model parameters (mean and standard deviation, SD) used in denitrification model and SMX degradation models. (*) Estimated from mean values.

	Organic matter oxidation due to denitrification processes							
	Reduction of nitrate to nitrite		Reduction of nitrite to dinitrogen gas		Reduction of nitrate to nitrite		Reduction of nitrite to dinitrogen gas	
	Barbieri experiment				Nödler experiment			
	Mean	SD	Mean	SD	Mean	SD	Mean	SD
K_{max} (molC$_{org}$/mol C$_x$ d)	19.0	3.6	11	1.1	2.0	0.8	2.0	0.5
k_{s,NO_3^-} (M)	1.0 x10^{-4}	5.6 x10^{-5}	-	-	3.0 x10^{-3}	8.3 x10^{-4}	-	-
k_{s,NO_2^-} $K_{s,NO2}$(M)	-	-	5.0 x10^{-4}	4.8 x10^{-4}	-	-	7.5 x10^{-4}	5 x10^{-4}
$k_{s,C_{org}}$ $K_{s\ Corg'}$ (M)	1.6 x10^{-1}	3.9 x10^{-2}	1.8 x10^{-2}	1.0 x10^{-2}	1.0 x10^{-1}	1.1 x10^{-2}	4.3 x10^{-2}	1.4 x10^{-2}
k_i (M)	-	-	5 x10^{-4}	7 x10^{-5}	-	-	3.5 x10^{-1}	3.0 x10^{-1}
	Abiotic degradation of SMX enhanced by co-metabolism (denitrification)							
	Barbieri experiment				Nödler experiment			
	Mean		SD		Mean		SD	
k_1 (1/M^2 d)	6.0 x10^{14}		2.6 x10^{15}		2.0 x 10^{12}		9.97 x 10^{11}	
k_2 (1/M^2 d)	1.3 x10^{10}		6.8 x10^9		8.8 x 10^7		7.5 x 10^6	
k_3 (1/d)	4.93		2.88		0.39		0.108	
k_4 (1/M d)	9.2 x 10^6		3.8 x 10^5		2.1 x 10^6		4.11 x 10^5	
	Abiotic degradation of SMX enhanced by co-metabolism (iron reducing conditions)							
k_5 (1/d)	2.7							
k_6 (1/d)	0.96							
n	0.91							

The results of the calibration of the SMX degradation model are displayed in Table 3.4. The parameters inferred display a high degree of uncertainty, being larger in the BAR experiment. This is probably due to the lack of measurements regarding one of the metabolites (desamino-SMX). Furthermore, the correlation matrix displayed by PEST showed that there was no correlation among the parameters (all values were lower than 0.55, results not shown).

Note that despite modelling the same processes in the two experiments, the parameters determined in BAR and NDL are quite different being higher in the

former. All but first-order degradation rates (3rd-order in the nitrosation of the primary amines and 2nd-order in the nitration of the benzene ring) depend on initial conditions (Atkins and de Paula 2011). As the initial conditions were three orders of magnitude different, the parameters cannot be compared.

Regarding the degradation of SMX under iron-reducing conditions, the best fit (Figure 3.5) was obtained using the parameters automatically calibrated by PEST (Table 3.4). The fit with an exponential model is also presented, focusing on early time data, to show the behaviour transition as a function of time. Note that all potential degradation pathways described would be naturally limited by the low amount of organic carbon in the subsoil. Besides this, iron-reducing conditions would only be reached after all previous redox states ended. Thus, the amount of organic carbon supplied to the system will play an important role. Once iron reducing conditions were achieved, abiotic processes will be enhanced and the degradation of SMX was achieved in hours (Figure 3.5).
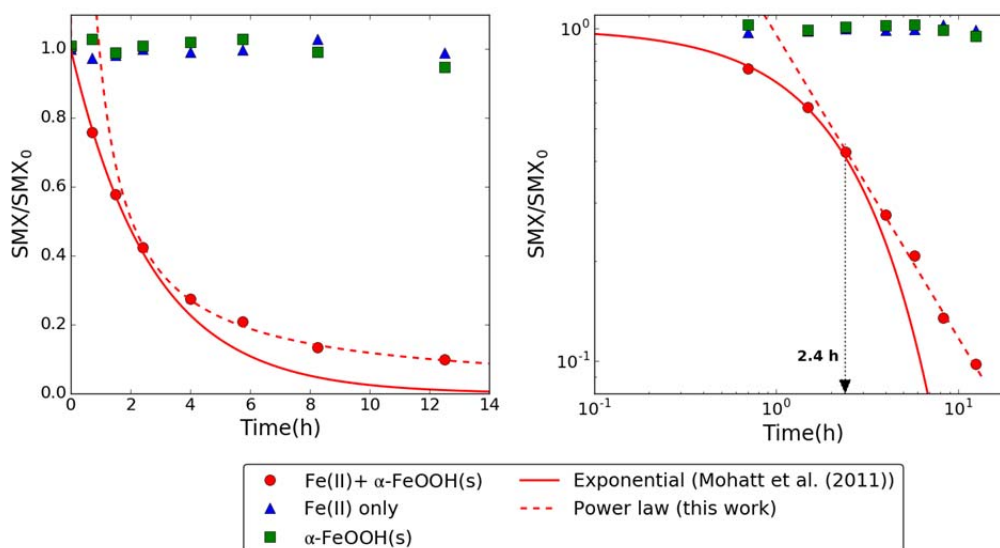

Figure 3.5. Experimental point (from Mohatt et al., 2011) and modelling results using first-order degradation rate and power law.

3.4.2. Potential extensions to real field site applications

The main reactive path for the degradation of SMX under denitrifying conditions involves the presence of nitrous acid that accumulates associated with the building up (and further decay) of nitrite. Nitrite is a usual transient compound in denitrification processes. Its accumulation is traditionally explained by a number of reasons: 1) the presence of low levels of oxygen; 2) the competition between nitrate and nitrite enzymes for a common electron donor; 3) large differences in the maximum reduction rates of nitrate and nitrite reductases; and 4) the choice of carbon source.

In addition, the presence of antibiotics is suggested to inhibit the reduction step from nitrate to nitrite in all denitrification process, and, thus, facilitate nitrite accumulation and nitrous acid formation. Other studies suggest that a continuous exposition to SMX in large quantities will affect the bacterial denitrifying community; consequently, the presence of 4-nitro-SMX would be quite plausible in natural aqueous environments where nitrate and antibiotics leakage converge. As the formation of desamino-SMX will be conditioned to the presence of alcohol which is not always present in organic matter, we expect that in real site applications 4-nitro-SMX will be the dominant metabolite.

3.4.3. Risk assessment

There is an increasing concern in the possibility that metabolites produced during the degradation of emerging compounds will be more hazardous to either human health or ecosystem than the parent itself. For that, we compared the LC50 for Daphnia sp. (after 48 h) and fish (after 96 h) calculated by ECOSAR packet of EPI-SUITE (USEPA 2012), for all the metabolites evaluated in this work. Both Daphnia sp. and fish were used as proxys of the full ecosystem. We included partition coefficients and solubility for each compound in order to compare the impact to the environment. Although the concentrations

of toxicity are referred to the acute toxicity and they are much higher than the environmental concentrations of SMX that serve as a comparative criterion.

Overall, 4-nitro-SMX was the most toxic compound (lowest LC50, see Figure 3.6). The toxicity was associated to the nitroaromatic compounds, acutely toxic and mutagenic, and many are suspected or established carcinogens. On the other hand, metabolites conserving the isoxazole ring (Product II and 3-amino-5-methylisoxazole) are more toxic when compared to SMX. Contrarily, 4-aminobenzosulfonate and metabolites produced under iron reducing conditions with broken isoxazole ring (Products III, IV) are the least toxic of all compounds, and can be mineralized easily. These results are correlated with values of log Kow and solubility; the highest values of the former correlated to the highest value of LC50, while the highest values of solubility correspond to low risk compounds. High solubility and low Kow values indicate that all the metabolites will remain mainly in water, with low absorptivity rates into solid phases.
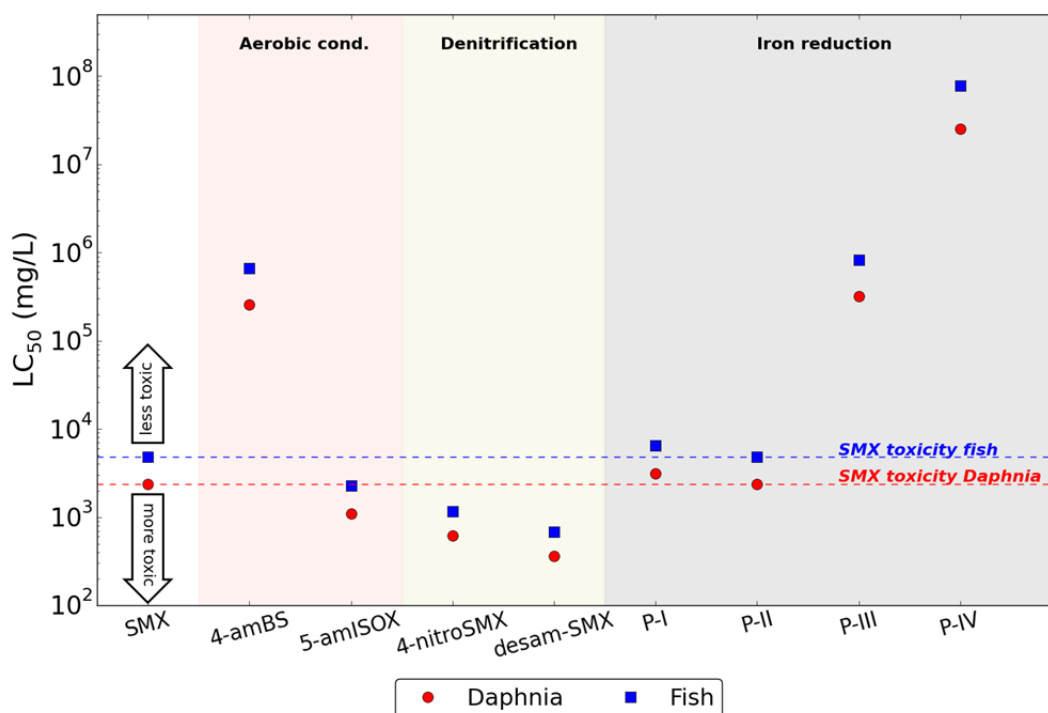

Figure 3.6. LC$_{50}$ of *Daphnia* (after 48 h) and fish (96 h) of SMX and its main metabolites under different redox conditions. 4-amBS and 5-amISOX are referred to aerobic metabolites 4-amino-benzolsulfonate and 3-amino-5-methyl-isoxazole LC$_{50}$ values were estimated using ECOSAR.

From the combination of reversibility and environmental fate/risk, it seems reasonable to conclude that the most efficient degradation path to remove all presence of SMX from groundwater bodies involves allowing the aquifer to reach iron reducing conditions. We want to stress here that this conclusion is only valid for SMX, and thus a potential intelligent methodology to eliminate a cocktail of emerging organic compound and their metabolites would be to allow the aquifer to reach many different redox states, each one of them being the most efficient one for the degradation of a given compound or metabolite. There is a need in the future to investigate many more molecules and even the synergic effect of injecting several compounds together.

3.5 Conclusions

We have conceptualized and modelled a comprehensive degradation path of the sulfamethoxazole molecule under different redox conditions in groundwater. We have developed a model capable of reproducing the fate of SMX as well as its metabolites under different redox conditions. Our model is based on the understanding of the real molecular mechanism of degradation instead of using simplified models postulating first-order degradation models, based on the apparent degradation behaviour of SMX in experiments.

Our model focused on denitrifying and iron-reducing conditions, being the dominant ones for SMX degradation in groundwater. The main reactive path for the degradation of SMX under denitrification involves the presence of nitrous acid, which promotes the nitrosation of the primary amine of SMX forming 4-nitro-SMX. If alcohol is present in the system a second metabolite is produced, desamino-SMX. Both of them are unstable and can eventually be retransformed to the parent compound. Biologically iron reduction conditions would facilitate the break of the SMX molecule through enhancing the abiotic mechanism of oxidation of ferrous iron to ferric iron. Several metabolites may be formed, involving the break of the isoxazole ring in the SMX molecule and individual potential degradation pathways.

The mathematical model proposed for SMX degradation under denitrifying conditions involves different forward and backward processes with complex kinetic rates. For 4-nitro-SMX two forward processes arise, one involving SMX and the concentration of HNO_2 squared, and a second one proportional to the concentration of desamino-SMX. The backward term implies linear first-order degradation. For desamino-SMX there is one forward term, proportional to the concentrations of SMX, HNO_2 and organic carbon in the form of alcohol, and a backward one proportional to the concentrations of desamino-SMX and HNO_3.

The model presented properly reproduced the results from two experiments reported in the literature. The actual parameters present in the governing equations are strongly influenced by the initial concentration of the SMX.

In the case of iron reducing conditions it was found that the best reproduction of a batch experiment is obtained by a combination of an exponential model at short times and a power law function at large times. The shortest reported characteristic time for degradation of the SMX molecule corresponds to iron reducing conditions. Further, it was found that the metabolites produced under iron reducing conditions are the most convenient in terms of minimizing total risk to ecosystems. The work performed regarding the fate of SMX could be extended to other EOCs, and each one of them is expected to behave differently and to be best degraded under specific redox conditions. Thus, in real field applications the optimal combination to degrade a suite of EOCs would be to enhance redox zonation by an engineered introduction of organic carbon in the aquifer.

References

Atkins, P., de Paula, J. (2011) Physical Chemistry for the life sciences. Second edition.

Banzhaf, S., Nödler, K., Licha, T., Krein, A., Scheytt, T. (2012) Redox-sensitivity and mobility of selected pharmaceutical compounds in a low flow column experiment. Sci. Total Environ. 438(0), 113-121.

Barbieri, M., Carrera, J., Ayora, C., Sanchez-Vila, X., Licha, T., Nodler, K., Osorio, V., Perez, S., Kock-Schulmeyer, M., Lopez de Alda, M., Barcelo, D. (2012) Formation of diclofenac and sulfamethoxazole reversible transformation products in aquifer material under denitrifying conditions: batch experiments. Sci. Total Environ. 426, 256-263.

Baumgarten, B., Jährig, J., Reemtsma, T., Jekel, M. (2011) Long term laboratory column experiments to simulate bank filtration: Factors controlling removal of sulfamethoxazole. Water Res. 45(1), 211-220.

Boetius A, Ferdelman T, Lochte K (2000) Bacterial activity in sediments of the deep Arabian Sea in relation to vertical flux. Deep Res II 47:2835–2875.

Bonin P, Omnes P, Chalamet A (1998) Simultaneous occurrence of denitrification and nitrate ammonification in sediments of the French Mediterranean Coast. Hydrobiologia 389:169–182.

Brune A, Frenzel P, Cypionka H (2000) Life at the oxic-anoxic interface: microbial activities and adaptations. FEMS Microbiol Rev 24:691–710.

Cardinale B, Srivastava D, Duffy J, et al. (2006) Effects of biodiversity on the functioning of trophic groups and ecosystems. Nature 443:989–92.

Carey, F.A., Sundberg, R.J. (2007) Advanced Organic Chemistry. Part B: Reactions and Synthesis., Springer.

Christy PM, Gopinath LR, Divya D (2014) A review on anaerobic decomposition and enhancement of biogas production through enzymes and microorganisms. Renew Sustain Energy Rev 34:167–173.

Choi K-H, Dobbs F (1999) Comparison of two kinds of Biolog microplates (GN and ECO) in their ability to distinguish among aquatic microbial communities. J Microbiol Methods 36:203–213.

Doherty, J. (2005) PEST: model independent parameter estimation. Watermark Numerical Computing, fifth edition of user manual.

Douterelo I, Goulder R, Lillie M (2011) Enzyme activities and compositional shifts in the community structure of bacterial groups in English wetland soils associated with preservation of organic remains in archaeological sites. Int Biodeterior Biodegradation 65:435–443.

Drillia, P., Dokianakis, S.N., Fountoulakis, M.S., Kornaros, M., Stamatelatou, K., Lyberatos, G. (2005) On the occasional biodegradation of pharmaceuticals in the activated sludge process: The example of the antibiotic sulfamethoxazole. J. of Hazardous Materials 122(3), 259-265.

Fernández-Turiel JL, Gimeno D, Rodriguez JJ, et al. (2003) Spatial and seasonal variations of water quality in a mediterranean catchment: the Llobregat river (NE Spain). Environ Geochem Health 25:453–74.

Fischer H, Kloep F, Wilzcek S, Pusch MT (2005) A River's Liver – Microbial Processes within the Hyporheic Zone of a Large Lowland River. Biogeochemistry 76:349–371.

Fischer H, Sachse A, Steinberg CEW, Pusch M (2002) Differential retention and utilization of dissolved organic carbon by bacteria in river sediments. Limnol Oceanogr 47:1702–1711.

Gao, J., Ellis, L.B.M., Wackett, L.P. (2010) The University of Minnesota Biocatalysis/Biodegradation Database: improving public access. Nucleic Acid Res 38(suppl 1), D488-D491.

Gao, S., Zhao, Z., Xu, Y., Tian, J., Qi, H., Lin, W., Cui, F. (2014) Oxidation of sulfamethoxazole (SMX) by chlorine, ozone and permanganate—A comparative study. J. Hazard. Mat. 274(0), 258-269.

Garland JL, Mills AL (1991) Classification and characterization of heterotrophic microbial communities on the basis of patterns of community-level sole-carbon-source utilization. Appl Environ Microbiol 57:2351–2359.

Gavrilescu, M., Demnerová, K., Aamand, J., Agathos, S., Fava, F. (2015) Emerging pollutants in the environment: present and future challenges in biomonitoring, ecological risks and bioremediation. New Biotechnol. 32(1), 147-156.

Ghiorse W, Wilson J (1988) Microbial ecology of the terrestrial subsurface. Adv Appl Microbiol 33:107–172.

Greskowiak J, Prommer H, Massmann G, Nützmann, G. (2005) The impact of variably saturated conditions on hydrogeochemical changes during artificial recharge of groundwater. Appl Geochemistry 20:1409–1426.

Greskowiak, J., Prommer, H., Massmann, G., Nützmann, G. (2006) Modelling seasonal redox dynamics and the corresponding fate of the pharmaceutical residue phenazone during artificial recharge of groundwater. Environ. Sci. Technol. 40(21), 6615-6621.

Griffiths RI, Whiteley AS, O'Donnell AG, Bailey MJ (2003) Influence of depth and sampling time on bacterial community structure in an upland grassland soil. FEMS Microbiol Ecol 43:35–43.

Göbel, A., Thomsen, A., McArdell, C.S., Joss, A., Giger, W. (2005) Occurrence and Sorption Behavior of Sulfonamides, Macrolides, and Trimethoprim in Activated Sludge Treatment. Environ. Sci. Technol. 39(11), 3981-3989.

Harvey HR, Tuttle JH, Bell JT (1995) Kinetics of phytoplankton decay during simulated sedimentation: Changes in biochemical composition and microbial activity under oxic and anoxic conditions. Geochim Cosmochim Acta 59:3367–3377.

Hedin LO, Von Fischer J, Ostrom N, et al. (1998) Thermodynamic constraints on nitrogen transformations and other biogeochemical processes at soil-stream interfaces. Ecology 79:684–703.

Hendel B, Marxsen J, Fiebig D, Preuss G (2001) Extracellular enzyme activities during slow sand filtration in a water recharge plant. Water Res 35:2484–8.

Kristensen E, Ahmed SI, Devol AH (1995) Aerobic and anaerobic decomposition of organic matter in marine sediment: Which is fastest? Limnol Oceanogr 40:1430–1437.

Liu, Y.-S., Ying, G.-G., Shareef, A., Kookana, R.S. (2013) Biodegradation of three selected benzotriazoles in aquifer materials under aerobic and anaerobic conditions. J. Contam. Hydrol. 151, 131-139.

Mohatt, J.L., Hu, L., Finneran, K.T., Strathmann, T.J. (2011) Microbially mediated abiotic transformation of the antimicrobial agent sulfamethoxazole under iron-reducing soil conditions. Environ. Sci. Tech. 45(11), 4793-4801.

Müller, E., Schüssler, W., Horn, H., Lemmer, H. (2013) Aerobic biodegradation of the sulfonamide antibiotic sulfamethoxazole by activated sludge applied as co-substrate and sole carbon and nitrogen source. Chemosphere 92(8), 969-978.

Nödler, K., Licha, T., Barbieri, M., Pérez, S. (2012) Evidence for the microbially mediated abiotic formation of reversible and non-reversible sulfamethoxazole transformation products during denitrification. Water Res. 46(7), 2131-2139.

Oliveira V, Santos AL, Coelho F, et al. (2010) Effects of monospecific banks of salt marsh vegetation on sediment bacterial communities. Microb Ecol 60:167–79.

Reis, P.J.M., Reis, A.C., Ricken, B., Kolvenbach, B.A., Manaia, C.M., Corvini, P.F.X., Nunes, O.C. (2014) Biodegradation of sulfamethoxazole and other sulfonamides by Achromobacter denitrificans PR1. J. Hazard. Mat. 280(0), 741-749.

Rodríguez-Escales, P., van Breukelen, B., Vidal-Gavilan, G., Soler, A., Folch, A. (2014) Integrated modeling of biogeochemical reactions and associated isotope fractionations at batch scale: A tool to monitor enhanced biodenitrification applications. Chem. Geol. 365(0), 20-29.

Romaní AM, Artigas J, Ylla I (2012) Extracellular Enzymes in Aquatic Biofilms: Microbial Interactions versus Water Quality Effects in the Use of Organic Matter. Microb. Biofilms. pp 153–174

Romani A, Sabater S (2001) Structure and activity of rock and sand biofilms in a mediterranean stream. Ecology 82:3232–3245.

Schaffer, M., Kröger, K.F., Nödler, K., Ayora, C., Carrera, J., Hernández, M., Licha, T. (2015) Influence of a compost layer on the attenuation of 28 selected organic micropollutants under realistic soil aquifer treatment conditions: Insights from a large scale column experiment. Water Res. 74(0), 110-121.

Schwarzenbach, R.P., Escher, B.I., Fenner, K., Hofstetter, T.B., Johnson, C.A., von Gunten, U., Wehrli, B. (2006) The Challenge of Micropollutants in Aquatic Systems. Science 313(5790), 1072-1077.

Taylor J., Wilson B, Mills M., Burns R. (2002) Comparison of microbial numbers and enzymatic activities in surface soils and subsoils using various techniques. Soil Biol Biochem 34:387–401.

USEPA (2012) Estimation Programs Interface Suite™ for Microsoft® Windows.